



RESEARCH & DEVELOPMENT

Reasonable Alternatives for Grade-Separated Intersections

**Institute for Transportation Research & Education,
North Carolina State University:**

Thomas Chase, MSCE, P.E.

Chris Cunningham, MSCE, P.E.

Shannon Warchol, MSCE, P.E.

Chris Vaughan, MSCE, P.E.

Taehun Lee

NCDOT Project 2018-20:

July 2020

Technical Report Documentation Page

1. Report No. NCDOT/NC/2018-20	2. Government Accession No.	3. Recipient's Catalog No.	
4. Title and Subtitle Reasonable Alternatives for Grade-Separated Intersections		5. Report Date July 13, 2020	
		6. Performing Organization Code	
7. Author(s) Thomas Chase, Chris Cunningham, Shannon Warchol, Chris Vaughan, Taehun Lee		8. Performing Organization Report No.	
9. Performing Organization Name and Address Institute for Transportation Research and Education North Carolina State University Centennial Campus Box 8601 Raleigh, NC		10. Work Unit No. (TRAVIS)	
		11. Contract or Grant No.	
12. Sponsoring Agency Name and Address North Carolina Department of Transportation Research and Analysis Group 104 Fayetteville Street Raleigh, North Carolina 27601		13. Type of Report and Period Covered Final Report August 2017 to July 2020	
		14. Sponsoring Agency Code NCDOT/NC/2018-20	
Supplementary Notes:			
16. Abstract Grade-separated intersections increase the capacity of two non-freeway roads by elevating two or more approaches, thereby removing conflict points. Over 150 grade-separated intersections exist today in North Carolina, with most designs utilizing interchange style ramps. The traditional interchange configurations have significant limitations in arterials where right of way is limited, freeway speeds are unsafe, and additional access is needed for bicycles, pedestrians and driveways. Additionally, the traditional Crash Modification Factor (CMF) preliminary safety analysis for intersections relies on pre-existing sites with a crash history to predict relative crash performance and the new designs are not yet built to develop these factors. The purpose of this study was to develop the operational and safety performance evaluation methods for grade-separated intersection designs and provide quantitative results for various traffic volume conditions. The outputs of this study are expected to be used as guidance for engineers and planners in choosing an appropriate design during the planning stage of a project. This study investigates the operational and safety effects of seven grade-separated intersection designs: direct left – downstream (DL-D), direct left – upstream (DL-U), single point left (SPL), three types of restricted crossing U-turn (RCUT (U-R), RCUT (R-U), and contra-RCUT), and quadrant - Southeast (QUA (SE)) intersection. Two existing alternative grade separated intersections are already available in CAP-X for alternatives analysis and do not fully grade separate the two arterial through movements for future conversion and therefore were not included in this study. This project developed seven new grade-separated intersection styles for the upper or lower half of the intersection design, resulting in over 40 new intersection designs in combination. These designs were analyzed for operational and safety performance with the creation of two new computational methods. The overall best design is entirely site specific and the planning level operational and safety models developed in this project can be used to identify preferred alternatives for a given volume condition.			
17. Key Words Grade-separated, Intersections, Operations, Safety		18. Distribution Statement	
19. Security Classif. (of this report) Unclassified	20. Security Classif. (of this page) Unclassified	21. No. of Pages 52	22. Price

Disclaimer

The contents of this report reflect the views of the authors and not necessarily the views of the Institute for Transportation Research and Education or North Carolina State University. The authors are responsible for the facts and the accuracy of the data presented herein. The contents do not necessarily reflect the official views or policies of the North Carolina Department of Transportation or the Federal Highway Administration at the time of publication. This report does not constitute a standard, specification, or regulation.

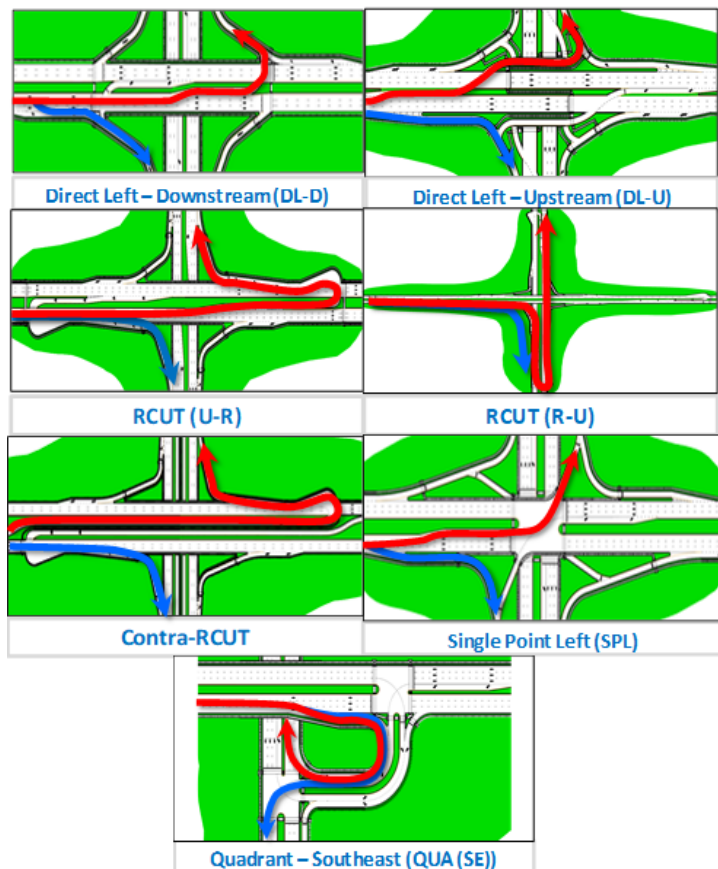
Acknowledgements

The research team acknowledges the North Carolina Department of Transportation for supporting and funding this project. We extend our thanks to the project Steering and Implementation Committee: Chair – Joseph Hummer, Research Engineers – Lisa Penny and Stephen Bolyard, Members – Kevin Lacy, Katie Hite, James H. Dunlop, Brian Mayhew, Michael P. Reese, Daniel Carter, and Brian Murphy.

Executive Summary

Grade-separated intersections increase the capacity of two non-freeway roads by elevating or depressing one or more approaches or movements, thereby removing conflict points. Despite not including a freeway, most of the grade-separated intersections are designed using freeway-level concepts such as loop ramps. While sometimes efficient, this sometimes results in excessive right-of-way needs, increased instances of pedestrians crossing free-flow movements, and over-design. Instead of using freeway-level design concepts, careful consideration of the means by which a vehicle can turn left across opposing traffic can result in more appropriate grade-separated intersections. However, the operational and safety performance for different designs of grade-separated intersection have not been fully investigated and compared in previous research.

The purpose of this study was to develop the operational and safety performance evaluation methods for grade-separated intersection designs and provide the quantitative comparison results for various traffic volume conditions. This study investigated the operational and safety effects of seven grade-separated intersection designs: direct left – downstream (DL-D), direct left – upstream (DL-U), single point left (SPL), three types of restricted crossing U-turn (RCUT (U-R), RCUT (R-U), and contra-RCUT), and quadrant - Southeast (QUA (SE)) intersection. The operational and safety performance on the major road for 16 volume scenarios are provided as output matrices, so that the users can combine the designs for major and minor roads for their needs. The seven designs are provided to the right for reference.



For the operational performance evaluation, this study used macroscopic and microscopic analysis to compare the designs. For the analysis, 16 volume scenarios were designed by a combination of different heavy traffic movements (e.g. heavy left turn, heavy through, normal, and so on) and approach volume proportions (e.g. EB : WB = 50% : 50% for balanced volume scenarios). The critical movement analysis method was used to compute and compare the v/c ratios for the macroscopic analysis. Prior to the microscopic analysis, some designs were grouped as they have similar operational features and similar trend in operational performance change over 16 volume scenarios. The microscopic analysis was conducted for the five representative designs: DL-D, SPL, RCUT (U-R), RCUT (R-U), and QUA (SE). For the microscopic analysis, the microscopic simulation tool VISSIM 10.0 was used to compare the operational performance of the designs between different volume scenarios. The simulation work was repeated 10 times for each scenario and the average delay was provided as a

performance measure for network level and the specific movements (e.g. Eastbound through and Westbound left turn) on the East-West (E-W) road. Both macroscopic and microscopic analysis showed the DL-D, SPL, and RCUT (U-R) have better performance than other designs overall. Also, all the designs commonly showed poor operational performance for the scenarios with heavy left turn traffics either on the Eastbound (EB) or Westbound (WB) approach. This result implied the overall performance of seven grade-separated intersection designs are significantly affected by the heavy left turn and the opposing through traffic movements.

For the safety performance comparison between All designs, there are several existing approaches, such as simple and weighted conflict point (CP) comparison methods, and the use of SPFs with the CMFs. However, the CP comparison methods cannot account for traffic volume, different crash rate and severity for CP types. Also, the SPFs have limitations in its application to the alternative intersections/interchanges (Alls) without reliable CMFs. Last, it requires significant time and effort to collect enough sample data to estimate reliable CMFs. To address the limitations of previous approaches, this study proposed a new safety method based on the movement-based safety performance functions (MB-SPFs). MB-SPFs have no limitation in application for any geometry of intersection because it separately predicts the conflict point (CP) and non-conflict point (NCP) crashes using two different models: CP-SPF and NCP-SPF. The heterogeneity in crash frequency and rate between CP types, crash data classification, model development and estimation, interpretation of results are discussed in this report. The predicted CP crashes on the major (E-W) road for 16 designed volume scenarios are provided as an output matrix for the seven intersection designs. The results showed RCUT (U-R), Contra-RCUT, and RCUT (R-U) relatively better safety performance than other designs overall.

This study also provides a summary of a patent landscape conducted by Innovate Carolina. It is notable that many of the results are patents and applications filed for China, Korea, and other Asian countries. This is a reasonable finding, given that they have a greater number of vehicles – plus bicycles and pedestrians – on their roads than we have in the US. The patent titles with the publication numbers found during the analysis are provided.

The outputs of this study are expected to be used as a guidance for engineer and planners in choosing an appropriate design when converting existing conventional intersections with heavy traffic congestion to an alternative design with a higher capacity. Overall, for intersections with heavy left turning volumes, the designs with upstream left turns or single point turns performed best. The overall best design is entirely site specific and the planning level operational and safety models developed in this project can be used to identify preferred alternatives for a given volume condition.

Table of Contents

Technical Report Documentation Page	2
Disclaimer	3
Acknowledgements	3
Executive Summary	4
Table of Contents	6
1 Introduction	9
1.1 Need Definition	9
1.2 Research Scope and Objectives	9
1.3 Grade-Separated Intersection Designs	10
1.4 Organization of the Report	11
2 Patent Review	12
3 Qualitative Performance Measure Considerations	13
4 Operational Performance Evaluation	14
4.1 Introduction	14
4.2 Macroscopic Operational Analysis	14
4.2.1 Critical Movement Analysis	14
4.2.2 Analysis Scope for Operational Analysis	15
4.2.3 Scenario Design	16
4.2.3.1 Scenario Design Process	16
4.2.3.2 Turning Movement Volume Proportions for Scenarios	16
4.2.3.3 Volume Scenarios	17
4.2.4 Assumptions and Parameters for Analysis	18
4.2.5 Macroscopic Analysis Results	19
4.2.5.1 Analysis Results	19
4.2.5.2 Selection of Designs for Microsimulation	20
4.3 Microscopic Operational Analysis	22
4.3.1 Yellow and All-Red Intervals	22
4.3.2 Cycle Length and Phase Splits	23
4.3.3 Microscopic Analysis Scope	23
4.3.4 Results for Microscopic Analysis	24
5 Safety Performance Evaluation	28
5.1 Introduction	28

5.2	Literature Review	29
5.2.1	Conflict Point Comparison Method	29
5.2.2	Weighted Conflict Point Comparison Method - VJuST	30
5.2.3	Crash Modification Factor	31
5.2.4	Findings of Literature Review	32
5.3	Methodology	32
5.3.1	Model Development Process	32
5.3.2	Heterogeneity of Crashes	33
5.3.3	Concept of Movement-based SPFs	33
5.3.4	Crash Classification	34
5.3.5	Assignment of Crashes to Conflict Points	36
5.3.6	Conflict Movement Volume	36
5.3.7	Model Form Selection	37
5.3.8	Movement-Based SPFs	38
5.3.8.1	Conflict Point SPF	38
5.3.8.2	Non-Conflict Point SPF	39
5.4	Data Collection	39
5.4.1	Site Selection	39
5.4.2	Crash Data	41
5.4.3	Annual Average Daily Traffic (AADT)	41
5.5	Safety Analysis Results	42
5.5.1	Model Estimation Results	42
5.5.2	Cumulative Residuals (CURE) Plot	43
5.5.3	Crash Prediction Results for Designed Volume Scenarios	44
5.5.4	An Example of Crash Prediction Using MB-SPFs	45
5.5.4.1	Traffic Volume Inputs	45
5.5.4.2	Conflict Point Diagram	46
5.5.4.3	Conflict Movement Volumes	46
5.5.4.4	Crash Prediction	46
5.6	Limitations in Safety Analysis	48
5.6.1	Limitation in Crash Data Classification	48
5.6.2	Limited Sample Sites	48
6	Conclusions	48

6.1	Implementation and Future Research	49
	References	51

1 Introduction

1.1 Need Definition

Dozens of grade-separated intersections exist today in North Carolina. NCDOT is currently rebuilding at least one grade-separated intersection at Capital Boulevard and Peace Street in Raleigh, with several other intersections in need of rebuilding or consideration of grade separation where it currently does not exist. Grade-separated intersections increase the capacity of two non-freeway roads by elevating two or more approaches, thereby removing conflict points.

Despite not including a freeway, most of the grade-separated intersections are designed using freeway-level concepts such as loop ramps. While sometimes efficient, this often results in excessive right-of-way needs, increased instances of pedestrians crossing free-flow movements, and over design. For example, the interchange at NC-54 and U.S. 15-501 required approximately 500,000 square feet of right of way, while the physical intersection of the roads is less than 10% of that space. Considering there are more than 150 grade-separated intersections already in existence in North Carolina with others being considered, reducing right of way costs alone could save the state millions of dollars in land acquisition and court fees.

Instead of using freeway-level design concepts, careful consideration of the means by which a vehicle can turn left across opposing traffic can result in more appropriate grade-separated intersections. By avoiding freeway-level design techniques, right-of-way needs can be reduced by hundreds of thousands of square feet at each intersection. Speed control and metering of traffic in arterial networks is another benefit of implementing intersections on both grade-separated roadways. Full interchange designs also heavily impact access points for businesses and homes as well as pedestrian and bicycle crossing when incorporating free flowing vehicular movements. Therefore, to avoid installation of an inefficient design alternative, reliable guidance for the selection of appropriate designs for the grade-separated intersection needed to be developed.

1.2 Research Scope and Objectives

The purpose of this study was to develop the operational and safety performance evaluation methods for grade-separated intersection designs and provide quantitative results for various traffic volume conditions. The outputs from this study are expected to be used as guidance for engineers and planners in choosing an appropriate design during the planning stage of a project. This study investigated the operational and safety effects of seven grade-separated intersection designs: direct left – downstream (DL-D), direct left – upstream (DL-U), single point left (SPL), three types of restricted crossing U-turn (RCUT (U-R), RCUT (R-U), and contra-RCUT), and quadrant - Southeast (QUA (SE)) intersection. Two existing alternative grade-separated intersections are already available in CAP-X for alternatives analysis and do not fully grade separate the two arterial through movements for future conversion and therefore were not included in this study. In order to provide an engineer or planner the most flexibility during concept or design stages of a project, our study provided the operational and safety analysis results only for one of the two roads (e.g. major (E-W) road) that could intersect.

For the operational performance evaluation, this study used macroscopic and microscopic analysis to compare the operational performance between designs. The critical movement analysis method was used to compute and compare the v/c ratios for the macroscopic analysis. The microscopic simulation analysis was used to compare the average delay between the designs. For the safety

evaluation, this study developed and estimated a novel crash prediction methodology – movement-based safety performance functions (MB-SPFs) – which can be used for safety evaluation for any geometric configuration of an intersection.

1.3 Grade-Separated Intersection Designs

This section introduces the seven grade-separated intersection designs and their left turn treatments.

TABLE 1 summarizes the diagrams for the seven designs with the colored turning movements (left turning movement is red arrow, and right turning movement is blue arrow). For illustration purposes, major & minor roads designs are the same in the diagrams; however, they could be any combination of designs for the major and minor roads.

TABLE 1 GRADE-SEPARATED INTERSECTION DESIGNS AND TURNING MOVEMENTS TREATMENT

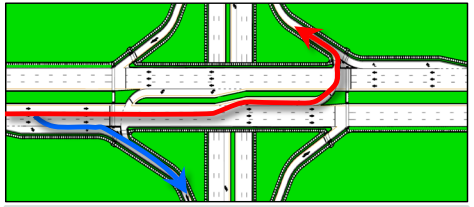
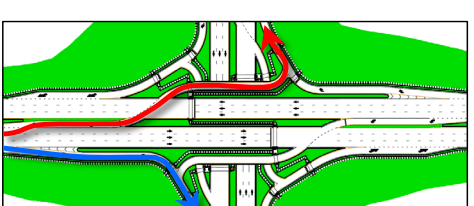
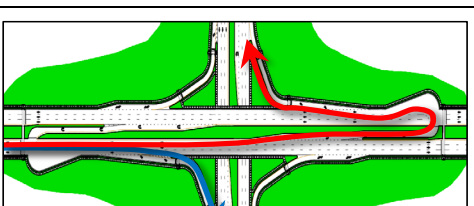
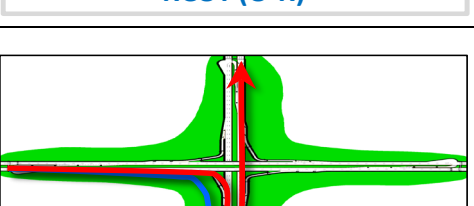
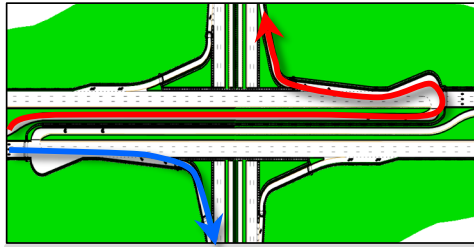
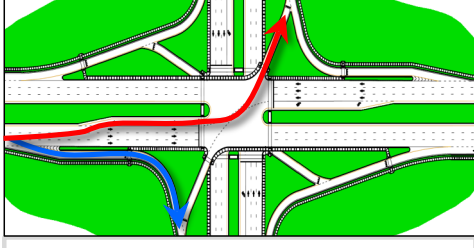
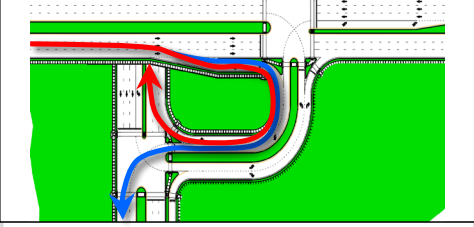
Diagram	Left Turn Treatment
 <p data-bbox="251 898 634 930">Direct Left – Downstream (DL-D)</p>	<p data-bbox="711 688 889 720">The left turn is</p> <ul data-bbox="760 730 1398 877" style="list-style-type: none"> • separated downstream of the signal on the major road • conflicting with opposing left turn and opposing thru
 <p data-bbox="251 1163 634 1194">Direct Left – Upstream (DL-U)</p>	<p data-bbox="711 953 889 984">The left turn is</p> <ul data-bbox="760 995 1360 1100" style="list-style-type: none"> • separated upstream of the signal on the major road • conflicting with opposing thru
 <p data-bbox="251 1436 634 1467">RCUT (U-R)</p>	<p data-bbox="711 1226 889 1257">The left turn is</p> <ul data-bbox="760 1268 1414 1415" style="list-style-type: none"> • separated downstream of the signal on the major road • conflicting with opposing U-turn and opposing thru at U-turn point on the major road
 <p data-bbox="251 1709 634 1740">RCUT (R-U)</p>	<p data-bbox="711 1499 889 1530">The left turn is</p> <ul data-bbox="760 1541 1414 1751" style="list-style-type: none"> • separated downstream of the signal on the major road and then detoured to the minor road • conflicting with opposing U-turn on the major road and the opposing thru at U-turn point on the minor road

Diagram	Left Turn Treatment
 <p data-bbox="358 506 527 537">Contra-RCUT</p>	<p data-bbox="711 239 889 264">The left turn is</p> <ul data-bbox="760 275 1386 426" style="list-style-type: none"> • separated upstream of the signal on the major road • conflicting with opposing thru at U-turn point on the major road
 <p data-bbox="318 833 568 865">Single Point Left (SPL)</p>	<p data-bbox="711 567 889 592">The left turn is</p> <ul data-bbox="760 602 1370 720" style="list-style-type: none"> • separated at the signal on the major road • conflicting with the opposing thru on the major road
 <p data-bbox="253 1123 633 1155">Quadrant – Southeast (QUA (SE))</p>	<p data-bbox="711 877 889 903">The left turn is</p> <ul data-bbox="760 913 1360 1031" style="list-style-type: none"> • separated upstream of the signal on the major road and then move to the right turn ramp • not conflicting with any movement <p data-bbox="711 1062 1370 1087">* There are three signal phases on major & minor roads</p>

1.4 Organization of the Report

This report contains five sections beginning with this introductory chapter summarized below for ease of navigation.

- Patent Review – presents a comprehensive review for the patent of grade-separated intersection designs.
- Qualitative Performance Measure Considerations – provides a comparison of design-related qualitative performance.
- Operational Performance Evaluation – provides literature review, volume scenario design, and analysis results for the macroscopic and microscopic analysis for operational performance evaluation.
- Safety Performance Evaluation – discusses the literature review for the state-of-the-practice safety evaluation approaches and their limitations followed by an explanation of the concept, development process, and estimation of movement-based safety performance functions for safety performance evaluation.
- Conclusions – discusses the findings of this study and additional performance measure considerations. The authors highly recommend leaving open Appendix A while reviewing the report in order to see the visual designs.

2 Patent Review

Many alternative intersections have been patented by individual designers. During the design phase of a project, an agency wishing to implement a patented design must pay a fee to the patent holder. Therefore, it is important to understand the patent status that may be employed by the Department. The research team contracted Innovate Carolina to conduct a “patent landscape” to provide this necessary information to future design teams. It is notable that many of the results are patents and applications filed for China, Korea, and other Asian countries. This is a reasonable finding, given that they have a greater number of vehicles – plus bicycles and pedestrians – on their roads than we have in the US. TABLE 2 shows a summary of the titles and publication numbers found during the analysis. Further details can be found in Appendix B. Overall, the review found that the Center Turn Overpass patent US5921701A was expired and there are potentially conflicting patents for the Echelon and single point over single point combination design though the team cannot make a legal determination independently. None of the other investigated designs appear to have conflicting patents, but the research team recommends any agency to conduct an internal legal review if they believe there are potential patents conflicting with a selected design.

TABLE 2 SUMMARY OF PATENT REVIEW

Publication Number	Title
KR899789B1	2-PHASE SIGNALIZED GRADE SEPARATED INTERSECTION SYSTEM
JP2006274782A	ROAD GRADE-SEPARATED INTERSECTION STRUCTURE EQUIPPED WITH BARRIER-FREE ROUNDABOUT
JP2006274793A	ROAD GRADE-SEPARATED INTERSECTION STRUCTURE EQUIPPED WITH BARRIER-FREE ROUNDABOUT
US20130279977A1	Weaving-free interchange with few bridges and exterior exits and entrances only
CA2736686A1	WEAVING-FREE INTERCHANGE WITH FEW BRIDGES AND EXTERIOR EXITS AND ENTRANCES ONLY
WO2012061925A1	WEAVING-FREE INTERCHANGE WITH FEW BRIDGES AND EXTERIOR EXITS AND ENTRANCES ONLY
US5921701A	Traffic interchange for use with intersecting city streets
CA2588576C	INTERSECTION SYSTEMS
CA21120A1	INTERSECTION SYSTEMS
AU1999010554A1	Intersection systems
KR247325B1	ROAD CROSSING SYSTEM
IL136067D0	INTERSECTION SYSTEMS

3 Qualitative Performance Measure Considerations

In addition to safety and operational impacts, the applicability of the designs will depend on other factors, as shown in TABLE 3. These performance measures include:

Pedestrian and Bicycle Accessibility (not included in the summary table) at the grade-separated intersections follow similar trends to their at-grade intersection counterparts. One major distinction which applies for all designs developed is the control for merging movements, where signalized or stop control allows for the highest accessibility for bicycles and pedestrians.

Frontage Impact quantifies the number of frontages which would be accessible to driveways (higher is better access). Frontages are most often rendered inaccessible due to grade changes along a ramp. Each intersection has eight possible frontages, two along each quadrant. The score indicates how many of the eight frontages would be accessible, assuming the same design is used on the bridge and below the bridge.

Constructability describes the ability of the grade-separated intersection to be constructed given an existing at-grade intersection (higher is better). This is a qualitative assessment of the relative impact of constructing the elevated portion of the design. All designs would likely have substantial impact to maintenance of traffic due to the need to construct a bridge and abutments, but this assessment considers that impact a given and focuses on relative differences between the designs.

Convertibility describes the ability of the grade-separated intersection to be converted into a full service-level interchange at a later point in time (higher is better). For purposes of the analysis, it is assumed that the service-level interchange will use tangent ramps (as opposed to loop ramps) for entry and exit movements. Most intersections have moderate convertibility due to the existing presence of ramps. Modifications would be needed to remove signal infrastructure and prohibit left turning movements.

Queue Storage Space describes the ability of the design to provide for large left or U-turn queues (higher is better). This rating considered the impact of designs which redirect left turns to complete right turns and assumes resulting right turn storage is unimpeded by upstream signals or bridges. Left turn queue storage impeded by queue storage needs in the opposing direction would receive a “low” rating, while designs without this conflict receive a “high”.

Longitudinal Space Needs considers the needs of the design for space upstream and downstream of the original intersection (higher needs more space). This has impacts for other intersections along the corridor. Intersections with a “high” rating may not be appropriate for areas with closely spaced intersections.

Lateral Space Needs considers the needs of the design for lateral space (higher needs more space). Intersections which receive a “high” rating may need additional bridge width. Intersections with a “medium” rating require additional median space (which tends to be less costly to acquire than additional bridge width). Intersections with a “low” rating require neither of these.

TABLE 3 PM CONSIDERATIONS MATRIX

Performance Measure	DL-D	DL-U	SPL	RCUT (U-R)	Contra-RCUT	RCUT (R-U)	QUA
---------------------	------	------	-----	------------	-------------	------------	-----

Frontage Impact	4	4	4	4	4	4	6
Constructability	Medium	Medium	Medium	Medium	Low	Medium	High
Convertibility	Medium	High	Medium	Medium	Medium	Medium	Low
Queue Storage Space	Low	Medium	Medium	Medium	High	Medium	Low
Longitudinal Space Needs	Low	High	Medium	High	High	High	Low
Lateral Space Needs	Low	High	High	Medium	Medium	Medium	Low

In summary, the grade-separated quadrant performs well in many categories aside from the difficulty in upgrading into a full interchange due to locating all the ramps in a single quadrant. The quadrant design may also have limited left turn storage when the ramp location moves the intersection to the “near” side approach. The single point design also provides good performance and can be converted to a SPU if the elevated arterial is the one to remain signalized. In general, for convertibility, it is preferable to elevate the narrower roadway under the assumption that it remains an arterial in the future. Overall, due to the design parameters established for selecting these combinations, the designs presented perform well in convertibility and many of the other categories can be used to select preferred designs when there are right of way restrictions. Not included in the analysis but important to note is that additional frontage or space needs can be mitigated by serving some movements through additional intersections in the roadway network.

4 Operational Performance Evaluation

4.1 Introduction

This study defined a grade-separated intersection as a junction of two crossing roads separated by elevating one or two approaches with through traffic movements that are interrupted at least once by the signal. Due to a vertical separation of the two roads, the grade-separated intersection can be designed to reduce the conflict points between traffic movements by physical separation while also considering a wide range of at-grade intersection alternatives for removing conflicts. In many cases, this would yield the operational and safety benefits compared to a conventional intersection. In this chapter, the critical movement analysis method is briefly reviewed, and the traffic volume scenario design method is described in detail. Also, this chapter discusses the macroscopic and microscopic operational analysis methods and compares the performance evaluation results between the seven grade-separated intersection designs for 16 volume scenarios. The detailed drawings for the seven designs are included in Appendix A.

4.2 Macroscopic Operational Analysis

4.2.1 Critical Movement Analysis

Based on national guidance, a minimum of three measures of effectiveness (MOEs) were suggested for the operational performance evaluation of signalized intersection: capacity and volume-to-capacity (v/c) ratio; delay; and queue length (*l*). Among the three MOEs, the Capacity Analysis for Planning of

Junctions (Cap-X) tool used the v/c ratio as an operational performance measure (2). In recent years, it has become one of the most commonly used tools for planning-level macroscopic assessment for the operational performance of intersection/interchange design. By using CAP-X, engineers can easily calculate the v/c ratio for an intersection design of interest or compare the v/c ratios between different designs for a given traffic condition, providing the basis for the user to select the right design or designs for future modeling efforts.

In CAP-X, the v/c ratios were calculated using the critical movement analysis method, which is an effective way to quickly estimate the overall performance of an intersection in terms of v/c ratios. The critical movement analysis identifies the set of movements that cannot time concurrently and require the most time to serve demand (3). The detail steps of critical movement analysis are as follows.

- Step 1) Identify traffic movements
- Step 2) Arrange the desired phasing plan
- Step 3) Determine the critical phase volumes
- Step 4) Calculate the sum of critical volumes
- Step 5) Calculate the intersection capacity
- Step 6) Determine critical v/c ratio
- Step 7) Determine the intersection status

4.2.2 Analysis Scope for Operational Analysis

In alternative intersections/interchanges (AIs), it is common that a design may have multiple signalized zones as shown in the FIGURE 1. By using multiple signals, traffic movements can be detoured and conflict points distributed, allowing for the operational and/or safety improvements. As such, CAP-X determines the “intersection’s” overall performance using the maximum v/c ratio across multiple signalized zones. Similarly, this study determined the overall performance of intersections using the maximum v/c ratio across the signalized zones on the East-West road. FIGURE 1 shows the road geometry, signalized zones on the major (E-W) road, and the turning movement routes from the minor (N-S) road of the DL-D design for the grade-separated intersection. *Note: For illustration purposes, major and minor roads designs are both DL-D; however, they could be any combination of designs for the major and minor roads.*

FIGURE 1 provides a visual of the left turn (red) and right turn (blue) movements as they merge with the major road at the downstream signalized zones. The critical movement analysis does not consider the impacts of merging traffic. It assumes the v/c ratios for two signalized zones on the major road are not affected by the turning movement volumes from the minor road, except for RCUT (R-U) and QUA (SE). For signalized merge movements, the signalized zone analyzed was assumed to be the controlling zone. Therefore, this study only considered the major (E-W) road traffic volumes when designing the volume scenarios. The volume scenario design will be discussed in detail in the following section. In the same context, the design of the minor road does not affect the performance of major road (assuming no queue spillback occurs). Therefore, as noted earlier, this study used the same design of the major road on the minor road in the macroscopic and microscopic analysis.

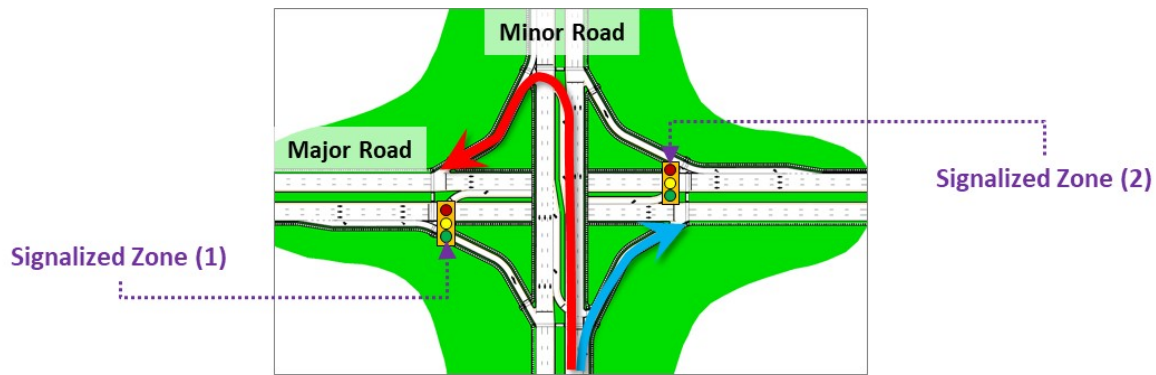


FIGURE 1 SIGNALIZED ZONES AND TURNING MOVEMENT ROUTES FROM MINOR ROAD (EXAMPLE DESIGN: DL-D)

4.2.3 Scenario Design

4.2.3.1 Scenario Design Process

Sixteen volume scenarios with different traffic volume conditions were designed in this study. The designed scenarios were used for the macroscopic and microscopic operational analysis as well as the safety performance comparison. The scenarios were designed using a combination of different proportions of turning movement (TM) volume (e.g. left turn, through and right turn movements) and different proportions of approach total volume (e.g. EB:WB = 50%:50% in balanced volume scenarios). Thus, the proportions of TM volume are consistent in both macroscopic and microscopic analysis, but the actual volumes are different.

The purpose of the macroscopic analysis was to compare the operational performance between intersection designs for a given traffic volume. As such, this study uses the same amount of total (EB+WB) volume of 6,500 vehicles per hour. This volume was chosen based on capacity calculations and provided an opportunity to differentiate designs based on operational performance between the seven intersection options explored in this project. On the contrary, the purpose of microscopic analysis was to compare the performance of an intersection design between different volume scenarios. Therefore, different total (EB+WB) volumes were used for each intersection design in the microscopic analysis. In the microscopic analysis, the turning movement volumes for scenarios were calculated by the total (EB+WB) volume, approach volume proportions (e.g. EB : WB = 50% : 50%), and the turning movement volume proportion (e.g. EB left turn = 15% of EB approach volume).

4.2.3.2 Turning Movement Volume Proportions for Scenarios

In designing the appropriate volume scenarios for analysis of different geometric designs, this study used TM count data collected from 84 approaches on 21 conventional four-leg signalized intersections in North Carolina. For each type of movement, the median, or 50th percentile, value of the 84 movement volumes was used for the typical traffic movement (low traffic). The third quartile, or 75th percentile, value was used for the heavy traffic movement (heavy traffic). For our analysis, the proportion was rounded up to the nearest 5% , and their values are shown in TABLE 4.

TABLE 4 TURNING MOVEMENT VOLUME PROPORTIONS FOR SCENARIOS

Heavy Movements Scenarios	Turning Movement Volume Proportion (%)		
	Left turn	Through	Right Turn
Normal	15	70	15
Heavy Left turn	30	60	10
Heavy Left turn + Thru	20	70	10
Heavy Thru	10	80	10

4.2.3.3 Volume Scenarios

The sixteen volume scenarios were designed based on the proportion of turning movement volumes. Each scenario represents a combination of the total approach volume condition (i.e. balanced and unbalanced volume conditions) and the heavy movement condition on the approaches (i.e. normal, heavy through, heavy through and left turn, and heavy left turn). Conceptually, 32 scenarios can be considered; however, this study selected 16 critical volume scenarios for the macroscopic and microscopic analysis. FIGURE 2 provides a visual representation of the framework for developing the volume scenarios.

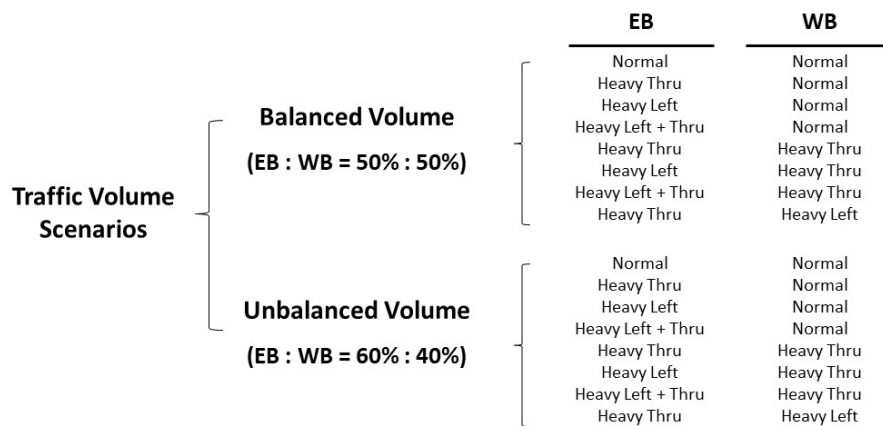


FIGURE 2 FRAMEWORK OF VOLUME SCENARIO DESIGN

The turning movement proportions and the traffic volumes for the macroscopic analysis were organized in TABLE 5. As stated earlier in this report, the critical movement analysis assumed the minor road volumes do not affect the operational performance of major road, except for the RCUT (R-U) and QUA (SE). Therefore, the sixteen volume scenarios had different volume conditions for turning movements on the major (E-W) road but consistent volume conditions for the turning movements on the minor (N-S) road.

Scenarios 1 - 8 are the balanced volume scenarios where the directional approach volume rates for EB and WB are 50% and 50%, respectively. Scenarios 9 - 16 are the unbalanced volume scenarios where the approach volume rates for EB and WB are 60% and 40%, respectively. The heavy movement column indicates the heavy movement scenarios defined in

TABLE 4. For example, 'EBN' indicates the normal (no heavy movement) scenario on the EB approach, and the 'WBL' indicates the heavy left turn scenario on the WB approach. The eight combinations of heavy movement scenarios for EB and WB approaches were designed to the balanced and unbalanced volume scenarios, respectively.

TABLE 5 DESIGNED VOLUME SCENARIOS FOR MACROSCOPIC OPERATIONAL ANALYSIS

Balanced Volume Scenarios (EB : WB = 50% : 50%)								Unbalanced Volume Scenarios (EB : WB = 60% : 40%)							
No	Heavy Movement	TM Proportions (%)			Traffic Volume (vph)			No	Heavy Movement	TM Proportions (%)			Traffic Volume (vph)		
		L	T	R	L	T	R			L	T	R	L	T	R
1	EBN	15	70	15	488	2275	488	9	EBN	15	70	15	585	2730	585
	WBN	15	70	15	488	2275	488		WBN	15	70	15	390	1820	390
2	EBT	10	80	10	325	2600	325	10	EBT	10	80	10	390	3120	390
	WBN	15	70	15	488	2275	488		WBN	15	70	15	390	1820	390
3	EBL	30	60	10	975	1950	325	11	EBL	30	60	10	1170	2340	390
	WBN	15	70	15	488	2275	488		WBN	15	70	15	390	1820	390
4	EBLT	20	70	10	650	2275	325	12	EBLT	20	70	10	780	2730	390
	WBN	15	70	15	488	2275	488		WBN	15	70	15	390	1820	390
5	EBT	10	80	10	325	2600	325	13	EBT	10	80	10	390	3120	390
	WBT	10	80	10	325	2600	325		WBT	10	80	10	260	2080	260
6	EBL	30	60	10	975	1950	325	14	EBL	30	60	10	1170	2340	390
	WBT	10	80	10	325	2600	325		WBT	10	80	10	260	2080	260
7	EBLT	20	70	10	650	2275	325	15	EBLT	20	70	10	780	2730	390
	WBT	10	80	10	325	2600	325		WBT	10	80	10	260	2080	260
8	EBT	10	80	10	325	2600	325	16	EBT	10	80	10	390	3120	390
	WBL	30	60	10	975	1950	325		WBL	30	60	10	780	1560	260

4.2.4 Assumptions and Parameters for Analysis

For the comparison of performance between intersection designs, this study made several assumptions for the macroscopic and microscopic analysis as follows.

- The volume adjustment factors for critical movement analysis were 0.95 for the left turn, 0.85 for the right turn, and 0.80 for the U-turn.
- The critical sum of 1,800 vph, 0% of trucks, and no U-turns were assumed in the analysis.
- Three lanes for the through movement and a single lane for turning (left, right, and U-turn) movements were used.
- In both the macroscopic and microscopic analysis, for all sixteen volume scenarios on the major road, the minor (N-S) road total volume was set to half of that of the major road.
- For the minor road, the normal turning movement condition (left turn of 15%, through of 70%, and right turn of 15%) was always assumed.
- In practice, four types of QUA intersection could be installed (e.g. QUA - Southeast, QUA - Southwest, QUA - Northeast, and QUA - Northwest). For given traffic condition, the engineers selected the most appropriate type unless there was any specific constraint. In light of this, the QUA (SE) was selected for the analysis since it shows relatively better performance for the sixteen volume scenarios. In this scenario, the heavy eastbound left turns right into the quadrant ramp and does not conflict with opposing westbound left and through traffic.

4.2.5 Macroscopic Analysis Results

4.2.5.1 Analysis Results

The purpose of conducting the macroscopic analysis was to compare the relative operational performance between the seven intersection designs using sixteen volume scenarios. The results are shown in the TABLE 6. The cells were colored according to their v/c ratios – deep green represents a relatively lower value and deep red represents the relatively higher value for the v/c ratio. Since the same total (EB+WB) volume of 6,500 vph was used for all the designs in the macroscopic analysis, it is appropriate to compare the performance for a scenario between intersection designs. The v/c ratios for the conventional four-leg signalized intersection are also provided as a reference. The detailed graphs for the comparison of performance between designs are provided in the appendix.

TABLE 6 MACROSCOPIC ANALYSIS RESULTS FOR 16 DESIGNED VOLUME SCENARIOS

Scenario	Approach Volume	Base	DL-D	DL-U	SPL	RCUT (U-R)	Contra-RCUT	RCUT (R-U)	QUA (SE)
		Conventional							
EBN-WBN	EB: 50% WB: 50%	0.85	0.80	0.71	0.71	0.94	0.85	0.77	1.28
EBT-WBN		0.91	0.83	0.77	0.77	0.94	0.88	0.77	1.34
EBL-WBN		0.99	1.08	0.99	0.99	1.28	1.19	0.77	1.22
EBLT-WBN		0.90	0.89	0.80	0.80	1.05	0.96	0.77	1.28
EBT-WBT		0.86	0.73	0.67	0.67	0.83	0.77	0.77	1.15
EBL-WBT		1.05	1.11	1.05	1.05	1.28	1.22	0.77	1.03
EBLT-WBT		0.96	0.92	0.86	0.86	1.05	0.99	0.77	1.09
EBT-WBL		1.05	1.11	1.05	1.05	1.28	1.22	0.77	1.53
EBN-WBN	EB: 60% WB: 40%	0.91	0.84	0.73	0.85	0.99	0.88	0.89	1.25
EBT-WBN		0.98	0.88	0.81	0.81	0.99	0.92	0.89	1.32
EBL-WBN		0.96	1.09	1.02	1.12	1.29	1.22	0.89	1.17
EBLT-WBN		0.91	0.88	0.79	0.96	1.02	0.95	0.89	1.25
EBT-WBT		0.94	0.80	0.73	0.81	0.90	0.83	0.89	1.17
EBL-WBT		1.01	1.12	1.07	1.12	1.29	1.25	0.89	1.02
EBLT-WBT		0.90	0.89	0.84	0.96	1.02	0.98	0.89	1.09
EBT-WBL		1.09	1.11	1.03	1.03	1.26	1.19	0.89	1.47

Overall, using the macroscopic analysis method, the DL-D, DL-U, SPL, and RCUT (R-U) showed better operational performance than the other designs. For the contra-RCUT, its relative rank between designs varied by scenario. It showed relatively better performance for the scenarios with the heavy

through movements both on the EB and WB approaches. The RCUT (R-U) showed constant performance for balanced and unbalanced volume scenarios since its v/c ratio for the E-W road was determined by the minor road turning movement volumes which are constant for balanced and unbalanced volume scenarios. Considering the results for RCUT (R-U) are based on the turning movement volumes from the minor road, the DL-D, DL-U, and SPL are recommended as the grade-separated intersection designs with better operational performance using the macroscopic analysis results. All designs had relatively poor performance for scenarios 3, 6, 8, 11, 14, and 16. Those scenarios commonly included a heavy left turn movement either on the EB or WB approach. This result implied the overall operational performances of seven grade-separated intersection designs are significantly affected by the heavy left turn and opposing through traffic movements.

4.2.5.2 Selection of Designs for Microsimulation

The purpose of microsimulation analysis was to compare the performance of seven grade-separated intersection designs using a diverse set of volume scenarios that could take place at any given intersection. Based on the macroscopic analysis, several intersection designs showed similar trends in performance across volume scenarios since they treat the left turn in similar ways. Therefore, in preparation for the microsimulation study, our team grouped designs by considering the operational features and the trend in v/c ratio from the macroscopic evaluation, allowing the simulation experiment to be significantly reduced in scale. The detailed intersection grouping process is described in the following sections.

DL-D and DL-U

Using the results from the macroscopic analysis, the research team determined that the DL-D and DL-U showed similar trends in v/c ratio change over the sixteen volume scenarios that were evaluated. In both designs, the intersection overall v/c ratio was determined by the left turn and opposing through traffic movements. Considering the similarity in the left turn treatment and the trends in performance, they were grouped and the DL-D was selected as a representative design for the microscopic analysis. The macroscopic analysis results for the two designs are visualized in FIGURE 3.

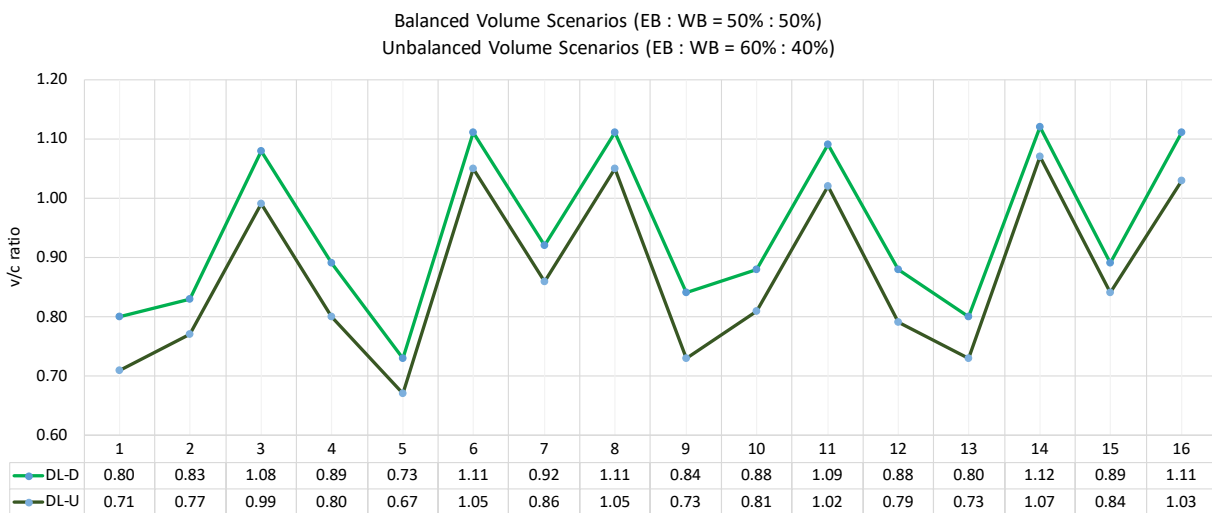


FIGURE 3 V/C RATIOS OF DL-D AND DL-U FOR 16 VOLUME SCENARIOS

RCUT (U-R) and Contra-RCUT

The RCUT (U-R) and contra-RCUT also had similar v/c ratios when looking at the sixteen volume combinations. In addition, the intersection v/c ratios were determined primarily using the through and left turn movements, which generate similar trends in operational performance. However, unlike the previous grouping, in these two designs the left turns are detoured and treated at the U-turn point and later merge with the opponent through movement. Therefore, these two intersections were grouped separately from the group of DL-D and DL-U.

FIGURE 4 shows the v/c ratios of two intersection designs over sixteen volume scenarios. Even though the location where left turn movement is separated from the through movement was different between two designs (downstream in the RCUT (U-R) and upstream in the contra-RCUT), the overall performance trend between volume scenarios was quite similar. Based on this, this study grouped them and used the RCUT (U-R) as a representative intersection for the microscopic analysis.

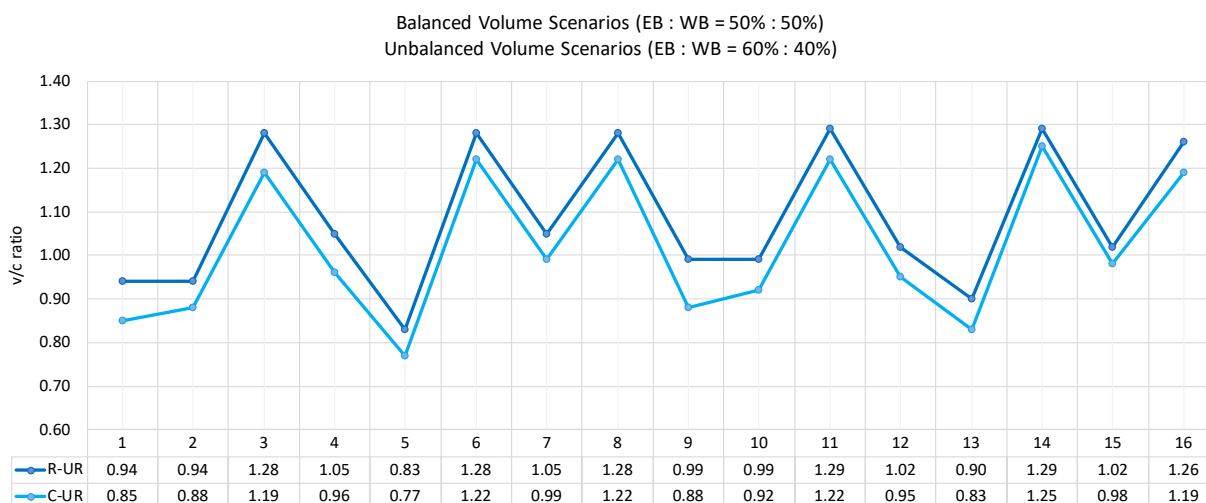


FIGURE 4 V/C RATIOS OF RCUT (U-R) AND CONTRA-RCUT FOR 16 VOLUME SCENARIOS

Through the intersection design grouping process, four designs were combined to two groups and the remaining three designs were singled out. The design grouping results are organized in the TABLE 7. In Section 4.3, the microscopic operational analysis results are provided for the five selected designs: DL-D, SPL, RCUT (U-R), RCUT (R-U), and QUA (SE).

TABLE 7 GRADE-SEPARATED INTERSECTION DESIGNS GROUPING RESULTS

	Seven Intersection Designs						
Before Grouping	DL-D	DL-U	SPL	RCUT (U-R)	Contra-RCUT	RCUT (R-U)	QUA (SE)
Grouped / Singled Out	Grouped		Singled Out	Grouped		Singled Out	Singled Out
After Grouping	DL-D		SPL	RCUT (U-R)		RCUT (R-U)	QUA (SE)

4.3 Microscopic Operational Analysis

4.3.1 Yellow and All-Red Intervals

For the microsimulation analysis, this study used the Highway Capacity Manual (HCM) method to calculate the appropriate cycle length and phase splits. Prior to the cycle length and phase splits computation, the yellow and all red intervals for the through and left turn movements were calculated using the following two equations suggested by the Institute of Transportation Engineers (ITE).

$$\text{Yellow Interval} = t + \frac{1.47S_{85}}{2a + (64.4 * 0.01G)} \quad (1)$$

Where

- t = driver reaction time (S);
- S_{85} = 85 percentile speed of approaching vehicles, or speed limit (mph);
- a = deceleration rate (fps);
- G = grade of approach (%); and
- 64.4 = twice gravitational acceleration of 32.2 fps.

$$\text{All Red Interval} \geq \frac{W + L}{1.47S_{15}} \quad (2)$$

Where

- S_{15} = 15th percentile speed of approaching vehicles, or speed limit (mph);
- W = distance from the departure stop line to far side of the farthest conflicting lane (ft); and
- L = length of a standard vehicle, usually taken to be 18 to 20 ft.

The parameters used in the above two equations are as follows.

- Approaching speed = 40 mph for a through movement, and 20 mph for a left turn movement
- Driver reaction time = 1 sec
- Deceleration rate = 10 fps
- Approach grade = 0 %
- Standard vehicle length = 18ft
- Intersection width = 40ft for a left turn movement / 30ft for a through movement

In equation (2) for the all red interval, the intersection width for a left turn movement was set at 40 feet as the movement crosses three lanes of opposing through traffic lanes. Likewise, for a through movement, the intersection width was set at 30 feet. As suggested in the MUTCD, the yellow interval was limited to between 3 and 6 seconds, and the all-red interval was limited to under 6 seconds. According to the equations above, this study used a yellow of 3 sec and all red of 2 sec for the left turn movement and a yellow of 4 sec and all red of 1 sec for the through movement.

4.3.2 Cycle Length and Phase Splits

Based on the yellow and all red intervals, our team determined the cycle length and phase splits by following the HCM method. In the microscopic analysis, the total (EB+WB) volume that satisfies the v/c ratio of 0.65 for the base volume scenario with no heavy traffic movement (scenario 1: EBN & WBN) was determined for each design. In the cycle length computation, too high or too low of a total volume resulted in an infeasible cycle length calculation (i.e. shorter than 45 sec or longer than 180 sec). To minimize the cases with infeasible cycle length, the total (EB+WB) volume satisfying the v/c ratio of 0.65 was used in this study.

The cycle length and phase splits for the movements were computed by following the three equations below. The HCM recommends the target range (critical) v/c ratio of 0.80 to 0.90. This study used a target critical v/c ratio at 0.90 in the analysis which would be representative of a more saturated condition. For the computed cycle lengths, the minimum and maximum were limited between 45 sec and 180 sec, respectively, to avoid the infeasible cycle length problem.

$$X_c = \left(\frac{C}{C-L} \right) \sum_{i \in ci} y_{c,i} \quad (3)$$

$$C = \frac{LX_c}{X_c - \sum_{i \in ci} y_{c,i}} \quad (4)$$

$$g_i = \frac{v_i C}{N_i s_i X_i} = \left(\frac{v}{N_i s_i} \right)_i \left(\frac{C}{X_i} \right) \quad (5)$$

where,

- C = cycle length (s);
- L = cycle lost time (s);
- X_c = critical intersection v/c ratio;
- $y_{c,i}$ = critical flow ratio for phase i = $\frac{v_i}{N_i s_i}$;
- ci = set of critical phases on the critical path;
- X_i = v/c ratio for lane group i;
- v_i = demand flow rate for lane group i (vph);
- N_i = number of lanes in lane group i (ln);
- s_i = saturation flow rate for lane group i (vphpl); and
- g_i = effective green time for lane group i (s).

4.3.3 Microscopic Analysis Scope

This section discusses the microsimulation analysis for the five representative (seven total) intersection designs: DL-D, SPL, RCUT (U-R), RCUT (R-U), and QUA (SE). For the analysis, the microscopic simulation tool VISSIM 10.0 was used. In the microscopic analysis, the same design of major road was used for the minor road. The total volume of minor road was assumed half of the major road total volume, and the minor road always used the 'no heavy movement' volume scenario. These assumptions assured the minor road would not significantly affect the operational performance on the major road. In VISSIM, it is

possible to obtain the operational performance results for the entire network as well as for the specific movements through the use of a node. As our interest was to investigate the operational performance on the major road, the node was set for the major (E-W) road only as shown by the black box in FIGURE 5.

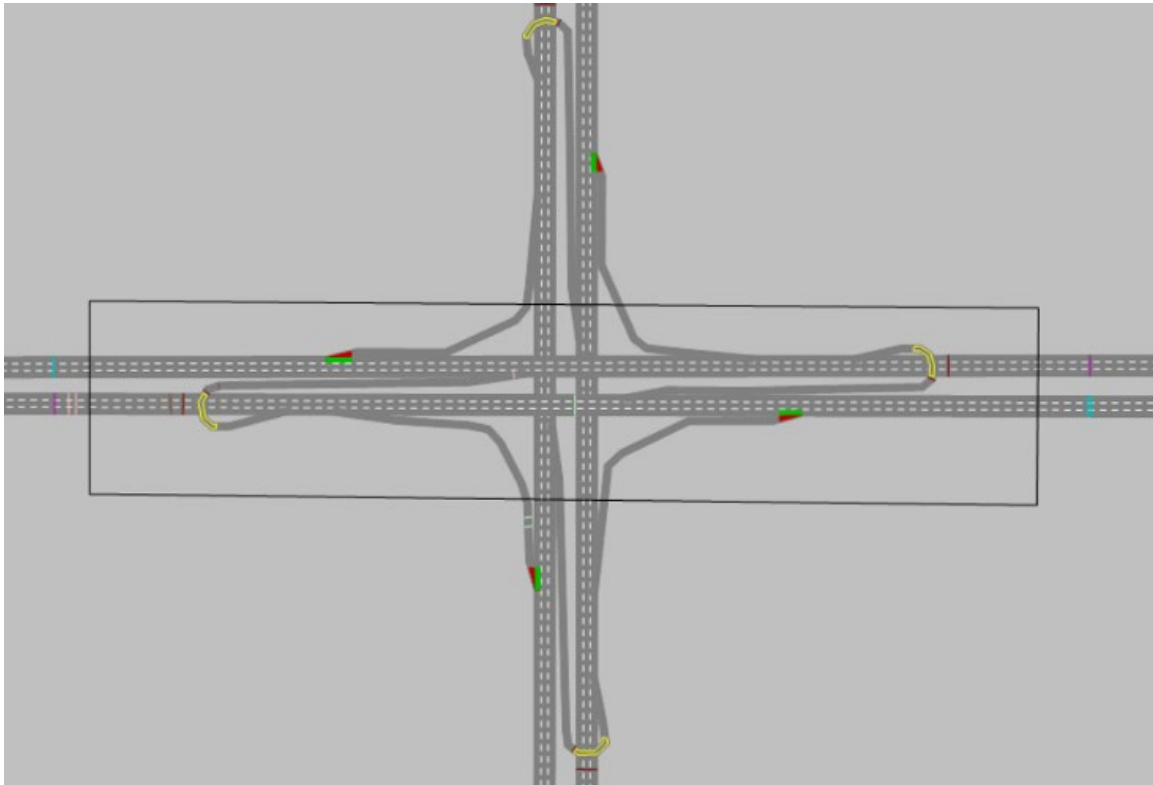


FIGURE 5 DATA COLLECTION NODE IN VISSIM ANALYSIS (EXAMPLE DESIGN: DL-D)

4.3.4 Results for Microscopic Analysis

The microscopic simulation analysis was repeated ten times for each scenario. The mean and standard deviation of average delay for ten simulated results are reported in the following two tables. Table 8 shows the results for the entire network and Table 9 shows those for the EB through and WB left turn movements collected from the node.

Table 10 shows the network-level total travel time for the scenarios. As stated previously, the total (EB+WB) volumes were customized for each of the five designs to satisfy v/c ratio = 0.65 for scenario 1, the base scenario. Therefore, the team deemed it appropriate to compare the performance of each design between the volume scenarios. For example, all the designs, except for the QUA (SE), show an increase the average delay in scenarios 3, 6, 11, and 14. On the contrary, the QUA (SE) had a different trend in performance over the sixteen scenarios. This trend also differs from the v/c ratios in the macroscopic analysis.

TABLE 8 MICROSIMULATION ANALYSIS RESULTS - NETWORK LEVEL AVERAGE DELAY (UNIT: SEC/VEH)

Scenario		DL-D		SPL		RCUT (U-R)		RCUT (R-U)		QUA (SE)	
		Mean	SD	Mean	SD	Mean	SD	Mean	SD	Mean	SD
1	EBN-WBN	11	0	22	2	13	0	53	17	91	6
2	EBT-WBN	12	1	14	1	13	0	33	11	49	9
3	EBL-WBN	117	3	31	3	61	2	117	15	74	7
4	EBLT-WBN	17	1	18	1	16	0	90	12	65	14
5	EBT-WBT	9	0	11	0	10	0	14	1	27	9
6	EBL-WBT	68	7	37	4	59	3	96	6	18	3
7	EBLT-WBT	18	1	25	3	15	0	69	5	18	3
8	EBT-WBL	69	8	40	4	58	1	108	11	90	12
9	EBN-WBN	46	9	22	1	14	2	82	7	88	7
10	EBT-WBN	11	0	15	1	11	0	35	11	58	12
11	EBL-WBN	125	8	27	0	94	1	150	24	64	11
12	EBLT-WBN	70	3	46	3	49	1	102	7	62	14
13	EBT-WBT	19	9	14	1	9	0	26	10	28	10
14	EBL-WBT	74	6	29	2	92	1	128	16	18	4
15	EBLT-WBT	50	1	44	1	47	1	92	5	21	5
16	EBT-WBL	40	13	35	5	44	1	160	41	98	4

TABLE 9 MICROSIMULATION ANALYSIS RESULTS - NODE (EBT & WBL) AVERAGE DELAY (UNIT: SEC/VEH)

Scenario		DL-D		SPL		RCUT (U-R)		RCUT (R-U)		QUA (SE)	
		Mean	SD	Mean	SD	Mean	SD	Mean	SD	Mean	SD
1	EBN-WBN	11	0	21	2	9	0	27	11	91	7
2	EBT-WBN	11	0	13	1	9	0	17	7	47	11
3	EBL-WBN	97	3	30	3	41	2	68	10	70	8
4	EBLT-WBN	16	1	17	1	11	0	51	8	62	14
5	EBT-WBT	8	0	10	0	7	0	9	0	23	8
6	EBL-WBT	56	6	36	4	40	2	60	5	13	3
7	EBLT-WBT	16	1	25	3	11	0	42	4	15	3
8	EBT-WBL	58	6	39	4	39	1	69	8	92	12
9	EBN-WBN	37	6	21	1	10	2	46	4	86	10
10	EBT-WBN	10	0	14	1	8	0	16	6	54	12
11	EBL-WBN	103	6	26	0	53	1	87	14	57	13
12	EBLT-WBN	55	2	45	3	29	0	58	3	55	14
13	EBT-WBT	17	7	13	1	7	0	14	5	22	9
14	EBL-WBT	60	5	28	2	52	1	80	10	13	3
15	EBLT-WBT	39	1	44	1	27	0	57	4	17	5
16	EBT-WBL	35	11	34	5	30	1	97	24	99	5

TABLE 10 MICROSIMULATION ANALYSIS RESULTS - NETWORK LEVEL TOTAL TRAVEL TIME (UNIT: SEC)

Scenario		DL-D		SPL		RCUT (U-R)		RCUT (R-U)		QUA (SE)	
		Mean	SD	Mean	SD	Mean	SD	Mean	SD	Mean	SD
1	EBN-WBN	525,000	9,000	494,000	19,000	506,000	7,000	951,000	132,000	478,000	11,000
2	EBT-WBN	528,000	10,000	419,000	10,000	500,000	7,000	798,000	87,000	346,000	36,000
3	EBL-WBN	1,124,000	14,000	566,000	31,000	847,000	24,000	1,258,000	93,000	446,000	24,000
4	EBLT-WBN	569,000	10,000	460,000	8,000	526,000	8,000	1,176,000	84,000	414,000	54,000
5	EBT-WBT	507,000	8,000	391,000	5,000	481,000	7,000	641,000	12,000	256,000	40,000
6	EBL-WBT	932,000	56,000	608,000	28,000	828,000	25,000	1,124,000	41,000	215,000	18,000
7	EBLT-WBT	577,000	13,000	525,000	29,000	521,000	7,000	1,026,000	34,000	216,000	18,000
8	EBT-WBL	942,000	66,000	633,000	29,000	825,000	17,000	1,212,000	80,000	471,000	46,000
9	EBN-WBN	760,000	58,000	483,000	8,000	508,000	15,000	1,069,000	52,000	467,000	21,000
10	EBT-WBN	521,000	7,000	427,000	10,000	488,000	6,000	820,000	90,000	398,000	53,000
11	EBL-WBN	1,180,000	50,000	501,000	7,000	958,000	11,000	1,335,000	139,000	403,000	40,000
12	EBLT-WBN	861,000	10,000	613,000	23,000	723,000	6,000	1,135,000	39,000	401,000	53,000
13	EBT-WBT	583,000	70,000	419,000	8,000	477,000	5,000	744,000	85,000	262,000	46,000
14	EBL-WBT	866,000	43,000	515,000	16,000	945,000	11,000	1,205,000	87,000	217,000	19,000
15	EBLT-WBT	773,000	6,000	600,000	11,000	703,000	5,000	1,067,000	24,000	231,000	25,000
16	EBT-WBL	748,000	107,000	600,000	38,000	723,000	15,000	1,581,000	208,000	516,000	13,000

* The figures in the table were rounded up to three places.

To investigate more deeply the results of the microsimulation analysis, the change rate of average delay and total travel time for sixteen scenarios were calculated based on the results in TABLE 8, TABLE 9 and TABLE 10. The change rate for the scenarios were organized in TABLE 11, TABLE 12, and TABLE 13, respectively. The figures in the tables show the relative change rate of average delay to Scenario 1. For example, the DL-D shows a 5% increased average delay in Scenario 2 compared to the base scenario (Scenario 1). The green cells indicate a change rate below 0%, the light yellow cells indicate a rate increase between 0 and 300%, and the red cells indicated a rate increase of more than 300%.

As the overall intersection performance was mainly determined by the EB through and the WB left turn movements, two tables show similar results in the change rate of average delay. In the TABLE 11, the DL-D and RCUT (U-R) showed more than 300% increase of network-level average delay in several scenarios, which include heavy left turn (or heavy left turn + thru) either on EB or WB approach. SPL, RCUT (R-U) and QUA (SE) showed relatively consistent performance across the sixteen volume scenarios. The change rates of node-level average delay showed similar results with network-level results. In contrast, the change rate of total travel time did not show significant difference between scenarios. This result implies the increased delay did not cause the significant increase in total travel time at the network-level.

It should be noted that the microscopic analysis was conducted with different amounts of traffic volumes for five designs. So, the results do not imply one design is better than another one for a certain scenario. Instead, the reader should understand some designs have more or less fluctuation in operational performance according to the traffic volume conditions. Even though DL-D and RCUT (U-R)

showed a significant increase in average delays, the total travel time showed much less difference between scenarios. Therefore, for DL-D and RCUT (U-R), it is recommended engineers investigate if turning movement proportions vary significantly by time of day or day of week for the heavy left turn movement.

TABLE 11 CHANGE RATE OF NETWORK-LEVEL AVERAGE DELAY (UNIT: %)

Scenario		DL-D	SPL	RCUT (U-R)	RCUT (R-U)	QUA (SE)
1	EBN-WBN	0	0	0	0	0
2	EBT-WBN	5	-37	-5	-37	-46
3	EBL-WBN	928	43	363	122	-19
4	EBLT-WBN	46	-17	18	71	-29
5	EBT-WBT	-20	-51	-24	-74	-70
6	EBL-WBT	494	68	343	83	-81
7	EBLT-WBT	53	16	14	32	-80
8	EBT-WBL	505	80	341	106	0
9	EBN-WBN	299	0	3	56	-3
10	EBT-WBN	-4	-34	-17	-33	-36
11	EBL-WBN	995	25	607	186	-29
12	EBLT-WBN	514	108	271	94	-32
13	EBT-WBT	65	-38	-28	-50	-69
14	EBL-WBT	551	31	594	144	-80
15	EBLT-WBT	341	100	254	75	-77
16	EBT-WBL	247	60	232	204	8

* Coloring criteria: Green = 0% or less, Light Yellow = between 0% - 300% increase, Red = more than 300% increase.

TABLE 12 CHANGE RATE OF NODE-LEVEL AVERAGE DELAY (UNIT: %)

Scenario		DL-D	SPL	RCUT (U-R)	RCUT (R-U)	QUA (SE)
1	EBN-WBN	0	0	0	0	0
2	EBT-WBN	4	-38	-6	-35	-48
3	EBL-WBN	818	42	338	156	-23
4	EBLT-WBN	47	-19	20	90	-32
5	EBT-WBT	-21	-52	-27	-66	-74
6	EBL-WBT	426	72	319	126	-85
7	EBLT-WBT	55	18	15	57	-84
8	EBT-WBL	451	85	317	160	2
9	EBN-WBN	252	0	9	71	-5
10	EBT-WBN	-5	-34	-18	-41	-40
11	EBL-WBN	870	24	460	227	-37
12	EBLT-WBN	425	115	204	116	-39
13	EBT-WBT	57	-38	-30	-48	-75
14	EBL-WBT	463	33	445	200	-85
15	EBLT-WBT	272	108	184	114	-81
16	EBT-WBL	228	64	213	261	9

* Coloring criteria: Green = 0% or less, Light Yellow = between 0% - 300% increase, Red = more than 300% increase.

TABLE 13 CHANGE RATE OF NETWORK-LEVEL TOTAL TRAVEL TIME (UNIT: %)

Scenario		DL-D	SPL	RCUT (U-R)	RCUT (R-U)	QUA (SE)
1	EBN-WBN	0	0	0	0	0
2	EBT-WBN	1	-15	-1	-16	-28
3	EBL-WBN	114	15	68	32	-7
4	EBLT-WBN	8	-7	4	24	-13
5	EBT-WBT	-4	-21	-5	-33	-46
6	EBL-WBT	77	23	64	18	-55
7	EBLT-WBT	10	6	3	8	-55
8	EBT-WBL	79	28	63	27	-1
9	EBN-WBN	45	-2	0	12	-2
10	EBT-WBN	-1	-14	-3	-14	-17
11	EBL-WBN	125	2	89	40	-16
12	EBLT-WBN	64	24	43	19	-16
13	EBT-WBT	11	-15	-6	-22	-45
14	EBL-WBT	65	4	87	27	-55
15	EBLT-WBT	47	22	39	12	-52
16	EBT-WBL	42	22	43	66	8

* Coloring criteria: Green = 0% or less, Light Yellow = between 0% - 300% increase, Red = more than 300% increase.

5 Safety Performance Evaluation

5.1 Introduction

Although the operational performance of Alternative Intersections/Interchanges (AIs) have been investigated through many prior efforts, the safety impacts of many have yet to be fully investigated. In trying to support engineers and planners to select an appropriate intersection design for a site, it is essential to provide quantitative analysis results to compare the relative safety performance between All designs. However, due to the different designs of AIs, the traditional Safety Performance Function (SPF) are not applicable to the safety evaluation of AIs. Therefore, state-of-the-practice planning level safety comparison methods are limited to simply comparing conflict points (CPs) between All designs by type (crossing, diverging, and merging) and overall (4). However, this is not a robust safety evaluation method as it cannot account for exposure due to varying traffic volumes or the inherent crash risk based on the varying CP types.

To improve on these known limitations, this study proposes a new concept of crash prediction using “movement-based” safety performance functions (MB-SPFs). The MB-SPFs have no limitation in applications for any geometry of intersection because it separately predicts the conflict point (CP) and non-conflict point (NCP) crashes in the two different models: CP-SPF and NCP-SPF. In this chapter, the commonly used safety evaluation methods and their limitations for application to AIs are discussed. Also, the concept of MB-SPFs are proposed and improvements on the limitations of the existing methods are discussed. The model development process and estimation results are also provided. Last, the predicted CP crashes for sixteen designed volume scenarios are compared between the seven intersection designs.

5.2 Literature Review

5.2.1 Conflict Point Comparison Method

According to the Federal Highway Administration (FHWA), CPs can be classified into three types (crossing, merging, and diverging) by their conflicting movements and characteristics (5). A simple CP analysis method compares the increase or decrease of CPs in full and by CP type between All designs and regards the reduced number of CPs as the improved safety performance.

For example, shows CP diagrams and the corresponding number of CPs by type and total for the displaced left turn (DLT), conventional, and restricted crossing U-turn (RCUT) intersections. Using the CP comparison method, the RCUT is the safest and the DLT is the second best between the three intersection designs. As the conflicting characteristics and conflict-related movements are different, the crash rates and severity are different between CP types. However, the simple CP comparison method cannot account for the difference in crash rate and severity, and, thus, it is not a robust quantitative methodology.

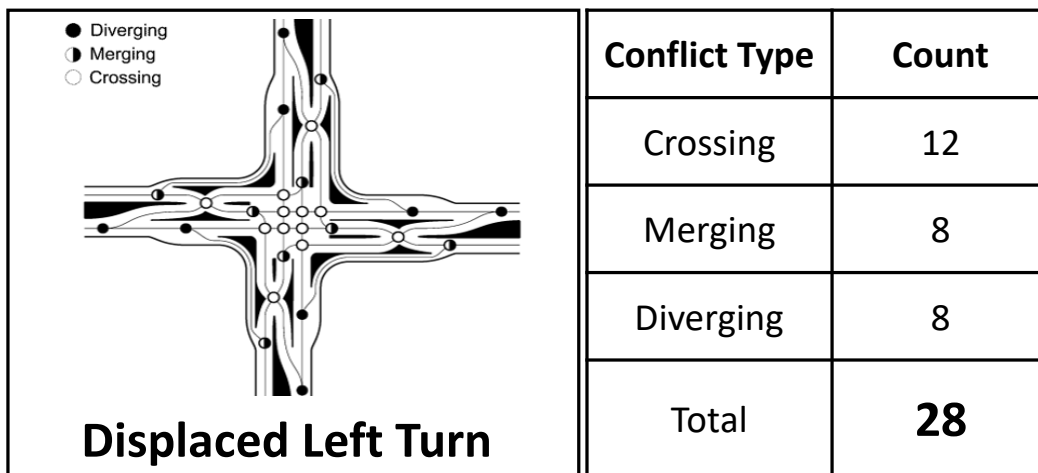


FIGURE 6 CONFLICT POINT DIAGRAM FOR DLT INTERSECTION

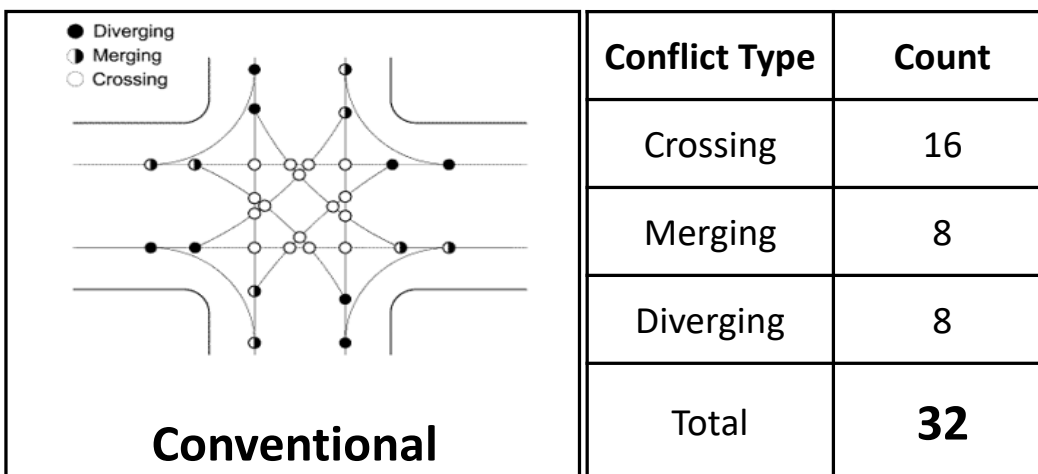


FIGURE 7 CONFLICT POINT DIAGRAM FOR CONVENTIONAL INTERSECTION

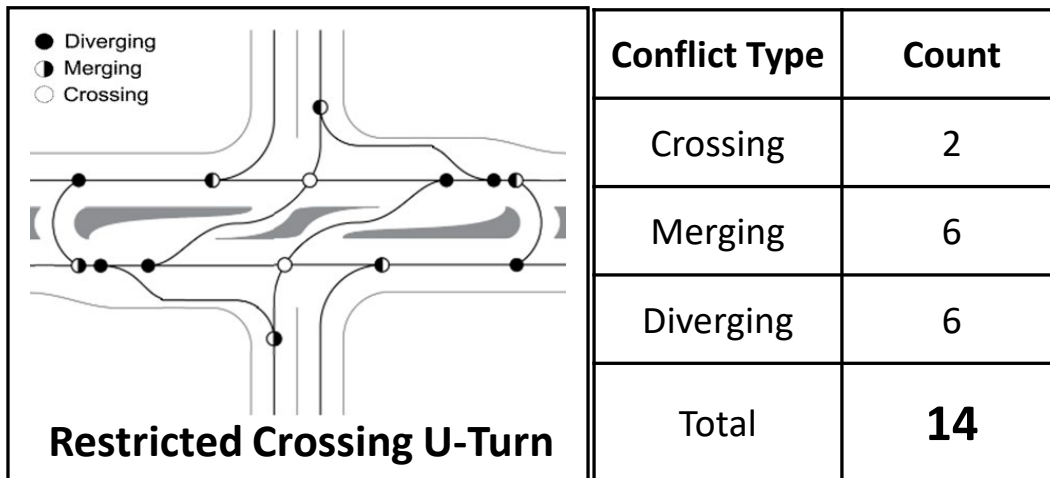


FIGURE 8 CONFLICT POINT DIAGRAM FOR RCUT INTERSECTION

5.2.2 Weighted Conflict Point Comparison Method - VJuST

To improve the limitations, the Virginia DOT used weighted CP totals as a relative safety measure for junction design. They developed the VDOT Junction Screening Tool (VJuST) for the planning level operational and safety performance evaluation. In the safety evaluation method of VJuST, they analyzed the total crash frequency for severities and CP types using the statewide crash data to calculate the weights for CP types. FIGURE 9 shows the safety evaluation process of the weighted CP comparison method in VJuST.

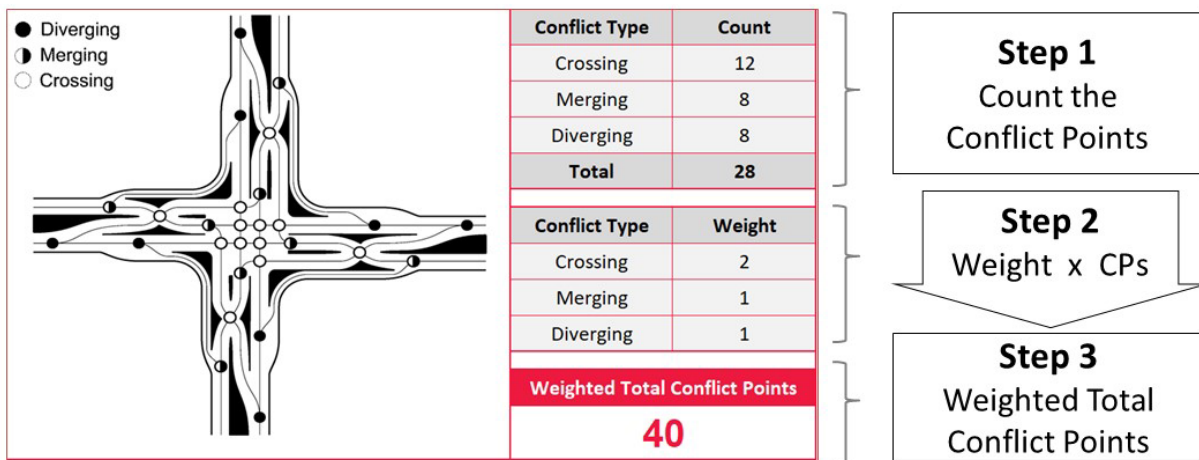


FIGURE 9. CONFLICT POINT COMPARISON METHOD IN VJUST

To simplify the crash classification, VJuST assumed the types of crashes that can occur for each type of CP. For example, head-on, angle, and sideswipe – opposite direction crashes were assumed to occur only at the crossing CPs, the sideswipe – same direction crashes occur only at the merging or diverging CPs. Next, the aggregated number of classified crashes was converted to average cost per crash for CP types, which then was converted using a weighting scheme. The weight factor for each type of conflict point was determined based on the average crash cost suggested in Highway Safety Manual

1st edition (6). The crash data in Virginia during five years from 2011 to 2015 in the calculation of weight factors. Last, they provide the weighted total CPs as the relative safety for intersection/interchange designs which can be compared amongst several design options.

- **Average Crash Cost by Severity (HSM, 1st Edition)**

- Fatal (K) Crash = \$4,008,885
- Disabling Injury (A) = \$216,059
- Evident Injury (B) = \$79,777
- Possible Injury (C) = \$44,868
- Property Damage (O) = \$7,428

As it is based on sufficient amount of crash records in Virginia, the weighted CP comparison method of VJuST primarily provides reasonable comparison results and is also easy to use in application. However, it still has limitations in that it cannot account for the impact of traffic volume on crashes and different crash rate for CP types. Moreover, the method considers the crashes occurred at CPs only and computes the weights for CP types based on the CP crashes. However, the statistics of crashes classified into CP and NCP crashes in this study showed a proportion of non-conflict point (NCP) crashes, such as rear-end or sideswipe crashes between the same or adjacent movements, is higher than that of CP crashes at an intersection (shown in TABLE 14). Therefore, the total (CP and NCP) crashes need to be used for the appropriate comparison of safety performance between All designs.

TABLE 14 CRASH FREQUENCY AND RATE FOR SEVERITY AND CP/NCP CRASHES

Crashes	Number of Crashes			FI Rate (%)	Average Crash Rate (crashes/year·million entering veh)		
	Total	FI	PDO		Total	FI	PDO
Total	1,838	566	1,272	30.8	0.651	0.225	0.426
NCP	1,275	321	954	25.2	0.434	0.125	0.309
CP Crashes	563	245	318	43.5	0.217	0.100	0.117
- Crossing	410	205	205	50.0	0.183	0.097	0.085
- Diverging	101	28	73	27.7	0.019	0.005	0.014
- Merging	52	12	40	23.1	0.047	0.012	0.035

* Note: the statistics in the table are based on the crash data in the section 5.4.2.

5.2.3 Crash Modification Factor

For planning level safety comparisons between Alls, engineers or planners may use the crash modification factor (CMF) developed for the installation of Alls (6). CMFs are the adjustment factors that can be multiplied to the expected crash frequency predicted by safety performance functions (SPFs). Using the safety performance functions (SPFs) with annual average daily traffic (AADT) volumes for major and minor roads at an intersection, users can estimate the expected crash frequency per year. Then, one or more CMFs can be multiplied to adjust the expected crashes for given characteristics of a site.

Despite the fact that CMFs are developed using a mathematically logical process, CMFs still have several difficulties in their development and use. A major difficulty in developing CMFs is collecting large enough sample of crash data for a sufficient period of time to show the difference in crash frequency

between before and after periods. For some All designs with limited numbers of installed sites, the problem could be even worse. Furthermore, it may require several years of data following the installation of an All to avoid regression-to-the-mean bias. For this reason, only a few CMFs have been developed for All designs. Another practical problem of CMFs is the potential reliability problem in application. As CMFs are developed based on a sample of sites with specific conditions, they may produce unreliable estimation results, especially when they are applied to a site with quite different characteristics, such as traffic volumes. Therefore, it is necessary to develop a more useful methodology for engineers or planners to compare the safety performance between All designs for different traffic volume conditions.

5.2.4 Findings of Literature Review

There are several existing approaches for safety comparison between All designs, such as simple and weighted CP comparison methods and the use of SPFs with the CMFs. However, they have their own limitations, and, thus, they are not the best approach to compare the safety performance between All designs for different volume conditions. To address the limitations, this study proposes a new safety comparison method based on MB-SPFs which can provide a much more robust analysis of safety impacts – even though an All may not even be in service. The features of MB-SPFs, and its improvements to the existing methods, are summarized in FIGURE 10. The following sections will discuss model development and estimation process in further detail.

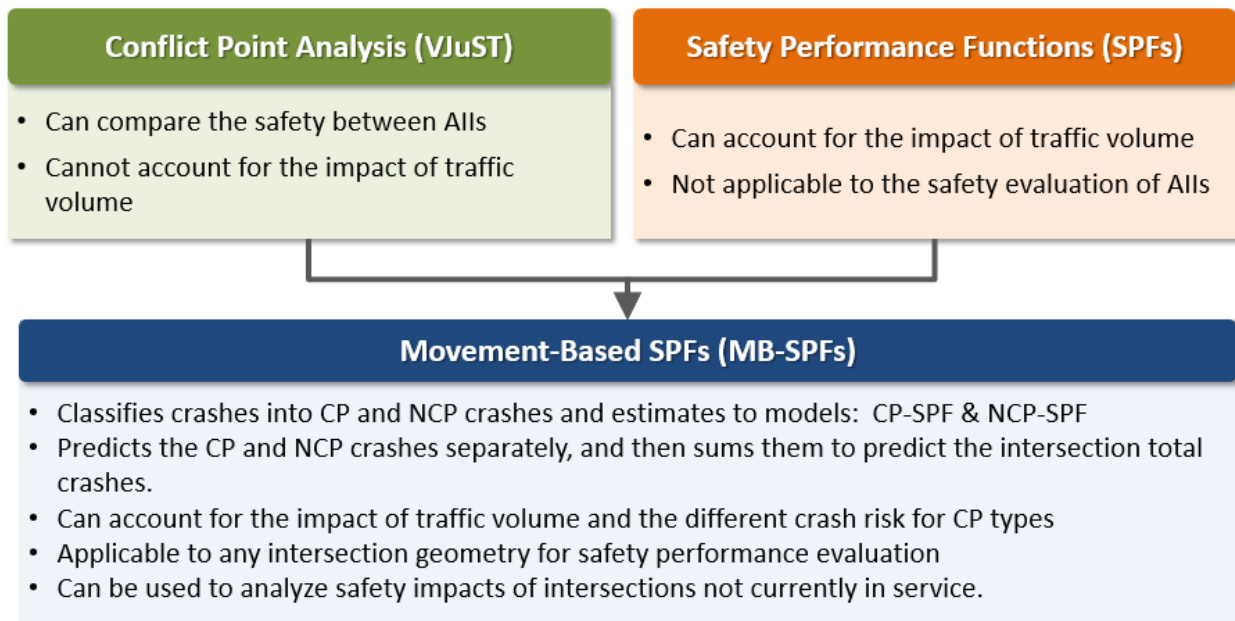


FIGURE 10 COMPARABLE FEATURES OF MOVEMENT-BASED SAFETY PERFORMANCE FUNCTIONS

5.3 Methodology

5.3.1 Model Development Process

This section discusses the model development process of MB-SPFs. First, the heterogeneity of crash frequency for severities are investigated, and the concept of MB-SPFs is proposed. Next, the research team expands on how the crashes are classified into CP and NCP crashes and how the CP crashes are assigned to the CPs. Last, the computation process for the conflict movement volumes (CMVs), model

form selection, and model specification of MB-SPFs are discussed, and concluded with a comparison of the relative safety performance comparison of grade-separated intersection designs.

5.3.2 Heterogeneity of Crashes

As a first step in development of MB-SPFs, this study investigated the heterogeneity of crash frequency for severities between CP and NCP crashes. In addition, variation in CP type was investigated. In this study, the CP crashes were defined as the crashes occurring between two conflicting movements at a CP (e.g. angle crashes between the Eastbound through and Westbound left turn movements). The NCP crashes were defined as the crashes occurring between same or adjacent movements (e.g. rear-end crashes between two vehicles in the Eastbound through movement). The crash classification method is demonstrated later in Section 5.3.4.

TABLE 14, noted earlier in Section 5.3.1, summarizes the crash frequency and crash rates for the 1,838 CP/NCP crashes used for the analysis in this study. The crash data were collected from conventional intersections and two types of Alls (e.g. RCUT or DDI). As the DDIs were interchanges including a freeway and an arterial road, the crashes occurring on the freeways were excluded from the analysis as they have quite different characteristics in the distribution of crash frequency. For the conventional intersections, to avoid sampling bias in traffic volumes, a similar number of sites were selected for different ranges of AADTs. As AADT is bi-directional, the average of major and minor AADTs in 2017 were considered. The selected sites include six intersections with average AADT under 10,000 veh/day, seven intersections with average AADT between 10,000 ~ 20,000 veh/day, and eight intersections with average AADT over 20,000 veh/day. The average crash rate in the table is the mean of yearly crash rates per million entering vehicles (MEV) for the intersections.

The summarized statistics in TABLE 14 show the crash frequency and rate for severity (total, fatal and injury (FI), and property damage only (PDO) crashes). The FI crashes include the severity K, A, B, and C, and the PDO crashes include the severity O and unknown severity. The analysis results showed the FI crash rates are similar in CP and NCP crashes as 0.100 and 0.125, respectively, while the total crash rate is higher in NCP crashes at 0.434 than that of CP crashes at 0.217. This is because the FI crash rate is significantly higher in CP crashes (43.5%) than the NCP crashes (25.2%). For CP crashes, the crash rate and FI rate are different between three CP types. All the total, FI, and PDO crashes show that the crossing CP, as you would expect, has higher average crash rates than diverging and merging. This result supports the appropriateness of crash classification using the CP and NCP crashes according to the conflicting movements.

5.3.3 Concept of Movement-based SPFs

Movement-based SPFs consist of two models: the CP- and NCP-SPFs. The CP-SPF predicts the CP crashes for a given CP, such as angle crashes between through and opposing turning movements. And the NCP-SPF predicts NCP crashes, such as rear-end or sideswipe crashes between same or adjacent movements, at the intersection-level. The basic concept of movement-based SPFs is illustrated in FIGURE 11.

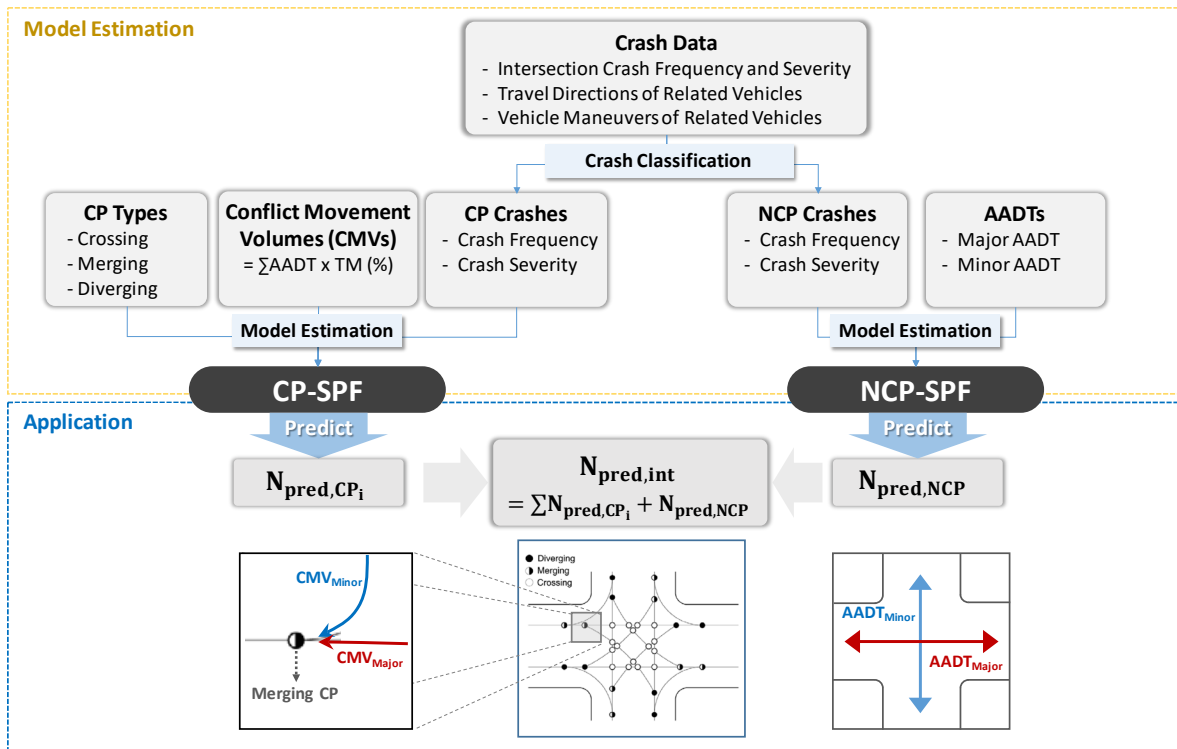


FIGURE 11 CONCEPT OF MOVEMENT-BASED SAFETY PERFORMANCE FUNCTIONS

Like the concept of a traditional SPF which predicts crashes by major and minor AADTs, the CP-SPF uses major and minor conflict movement volumes (CMVs) as exposure variables in the model. Each CP has two CMVs, one for each of the traffic movements passing the CP. The higher volume was set as the major CMV and the lower was set as the minor CMV. To account for the difference in crash rate and severity, the CP-SPF also uses the CP types (crossing, merging and diverging) as categorical variables. For model estimation of the NCP-SPF, the major and minor AADTs were used as exposure variables. In application, the predicted CP crashes were aggregated at the intersection-level and then added to the predicted NCP crashes to calculate the total expected crash frequency of an intersection.

5.3.4 Crash Classification

This study classified crashes into CP and NCP crashes based on the travel direction and vehicle maneuver information in the crash report. TABLE 15 shows crash patterns that can occur at each type of CP in the conventional four-leg signalized intersection. These crash patterns were the same as eight of the fifteen crash patterns by vehicle streams in the previous effort (7). And the other seven patterns were classified to the NCP crashes which is new to this particular study. The crashes not included in the CP crashes, which usually occur between vehicles in the same movement or adjacent movements on an approach (such as a rear-end crash), were classified as the NCP crashes. To avoid misclassification due to imprecise records for crash type, the crashes were classified based on the travel direction and vehicle maneuver information in the police crash report.

TABLE 15 CRASH CLASSIFICATION FOR CP TYPES IN CONVENTIONAL INTERSECTION

CP Type	Crash Patterns	Conflicting Movements for Crash Patterns
Crossing (16 CPs)		Pattern (a): Left turn & (same road) Opposing Through Pattern (b): Left turn & (different road) Through Pattern (c): Through & (different road) Through Pattern (d): Left turn & (different road) Left turn
Merging (8 CPs)		Pattern (e): Right turn & (different road) Through Pattern (f): Left turn & (different road) Through
Diverging (8 CPs)		Pattern (g): Left turn & (same road) Through Pattern (h): Right turn & (same road) Through

To classify crashes at the All sites, this study referred to the crash diagram in the safety project evaluation report for the sample sites. FIGURE 12 shows an example crash diagram for a crossover point in an RCUT in NC. As the conflicting movements and the crash location are clearly visualized in detail, it was easier to classify the crashes into CP/NCP crashes. Like a conventional intersection, the remaining crashes not included in the CP crashes were classified as NCP crashes. Similar to conventional intersections, most NCP crashes occurred between the same or adjacent movements on an approach.

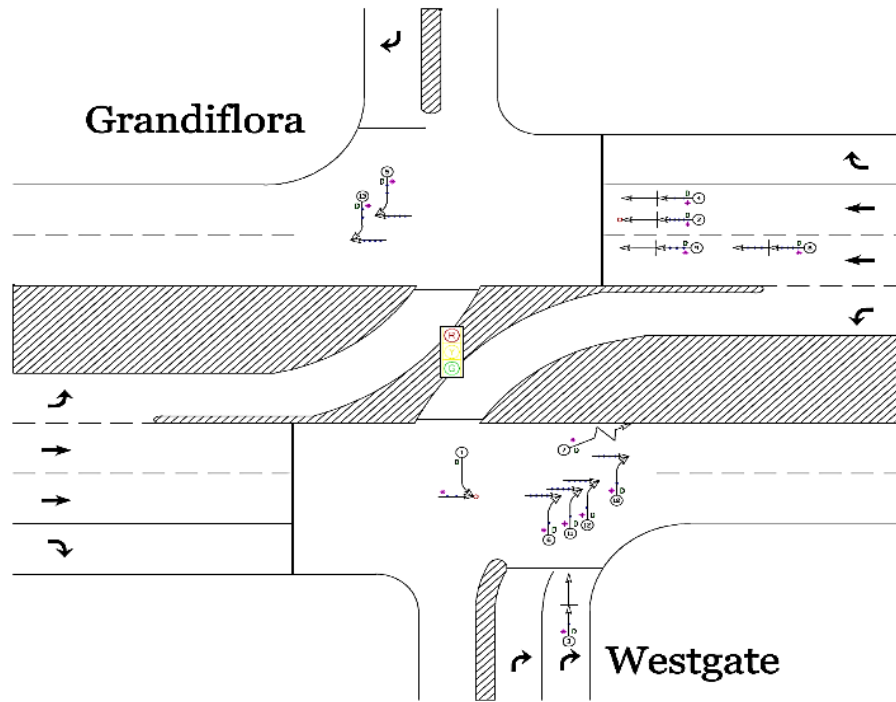


FIGURE 12 CRASH DIAGRAM IN THE SAFETY ASSESSMENT REPORT

SOURCE: US 17 SUPERSTREET BEFORE AND AFTER CRASH ANALYSIS SUMMARY, NC DOT.

5.3.5 Assignment of Crashes to Conflict Points

The conventional four-leg signalized intersection has 32 conflict points which are classified into three types: crossing (16 CPs), merging (8 CPs), and diverging (8 CPs) (8). On the contrary, AllIs have different numbers of total CPs based on the intersection design. For example, the DLT has 28 CPs, while the RCUT has 14 CPs. To identify the CPs and assign the crashes, the CP codes were created for the combinations of two movements conflicting at a CP. An example of CP codes for the RCUT is presented in FIGURE 13. For instance, in the middle of the figure, a crossing CP where the Eastbound left turn and Westbound through movements conflict was coded 'C1'. So, this study assigned CP codes to the collected CP crashes based on the travel direction and vehicle maneuver information recorded in the police crash report.

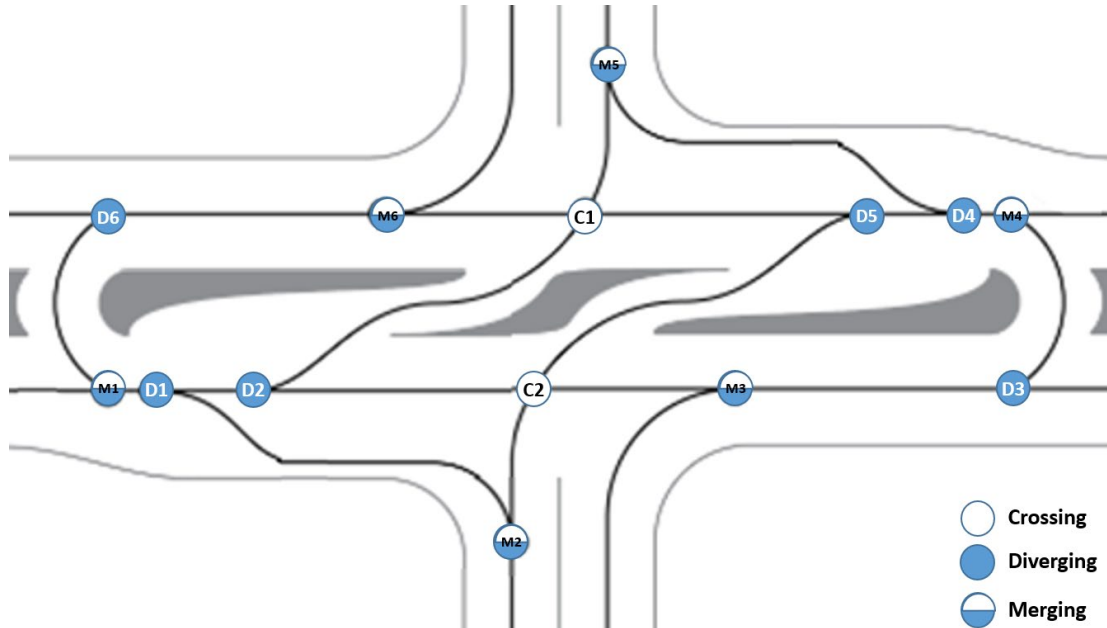


FIGURE 13 CONFLICT POINT CODES FOR RESTRICTED CROSSING U-TURN INTERSECTION

5.3.6 Conflict Movement Volume

The major and minor CMVs were computed for the model estimation of the CP-SPF. The CMVs were calculated by multiplying the sum of major and minor AADTs for each year, by the turning movement proportions (%) which were calculated from the turning movement counts, as shown in FIGURE 14.

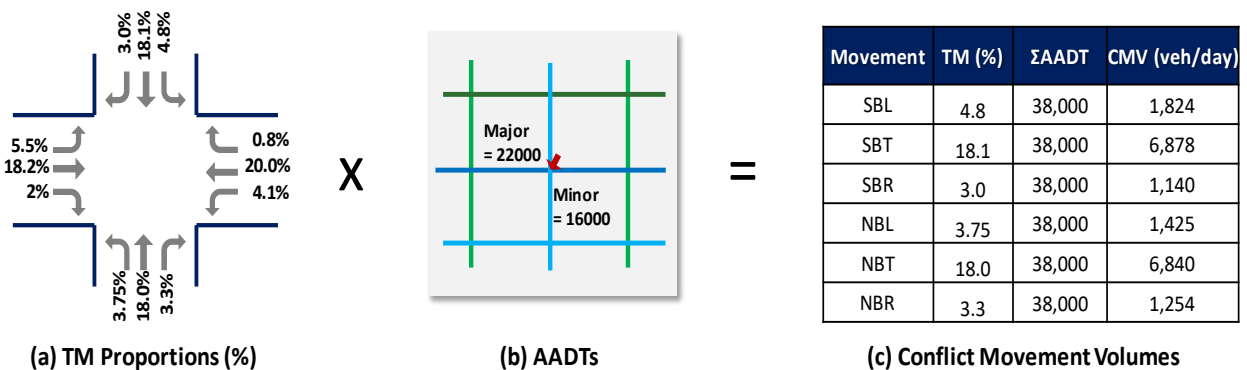


FIGURE 14 CONFLICT MOVEMENT VOLUME COMPUTATION PROCESS

These turning movement proportions are for a given movement out of the entire intersection traffic in contrast to typical turning movement percentages which are based on approach volume. The turning movement counts were observed for at least 11 hours and at most 16 hours a day – including the AM and PM peaks – in 2017 or the most recent year data was available. The calculated turning movement proportions were assumed to be consistent during the analysis periods since the available data was limited. To account for the year-by-year changes in traffic volumes, the yearly AADTs were multiplied by the turning movement proportions.

For Alls, the CMVs were determined by adding the detoured traffic volumes to the original movement volume. For example, at a crossing CP, which was coded as C1 in FIGURE 13, the actual conflicting movement volumes are EBL (eastbound left turn) and WBT+NBL (westbound through + northbound left turn). This is critical in evaluating the safety performance of Alls since they often remove CPs apart and make the turning movements detour to a separate intersection to improve operations. This produces an increase of conflicting movement volumes for a CP, causing higher expected frequency of crashes. Without this consideration of added volumes, it is likely to overestimate or underestimate the crash frequency for the Alls.

5.3.7 Model Form Selection

Crashes are inherently rare events and this aspect makes modelling especially challenging. Crash count data commonly shows overdispersion in the dataset where the observed variance is greater than the expected variance in the theoretical model (9). This overdispersion can also occur in crash data due to safety factors that are not considered in the model, unreliability in exposure data, and the heterogeneity in a highway environment (10).

Poisson and negative binomial regression models are most widely used for modeling rare event count data (11). However, the Poisson regression model is not appropriate for modeling over-dispersed count data since the model constrains the variance to be equal to the mean (11, 12). In this case, the negative binomial regression model can be used to handle the overdispersion problem in count data (13). The model form, mean, and variance of the negative binomial regression model with k independent variables for i observations are shown in the following three equations.

$$P(Y = y_i) = \frac{\Gamma(y_i + \alpha^{-1})}{\Gamma(\alpha^{-1})\Gamma(y_i + 1)} \left(\frac{1}{1 + \alpha\mu_i} \right)^{\alpha^{-1}} \left(\frac{\alpha\mu_i}{1 + \alpha\mu_i} \right)^{y_i} \quad (6)$$

where,

$$\mu_i = E(Y_i) = \exp(\alpha + \beta_1 x_{1i} + \beta_2 x_{2i} + \dots + \beta_k x_{ki}) \quad i = 1, 2, \dots, n. \quad (7)$$

$$Var(Y_i) = \mu_i + \alpha\mu_i^2 \quad (8)$$

The variance of the negative binomial regression model uses a dispersion parameter α . With $\alpha \geq 0$, the model can have a higher value of variance than the mean. When α approaches zero, the variance reduces to the mean and the negative binomial regression model approximates the Poisson

regression model (11). Therefore, the negative binomial regression model is more appropriate for modeling the over-dispersed count data as the model allows for a variance greater than the mean.

5.3.8 Movement-Based SPFs

Movement-based SPFs (MB-SPFs) consist of two models: the CP-SPF that predicts the CP crashes at the CP-level and the NCP-SPF that predicts the NCP crashes at the intersection-level. The expected number of crashes per intersection can be calculated by summing the aggregated CP and NCP crashes as shown in the equation (9).

$$N_{pred,int} = \sum_{i=1}^n (N_{pred,CP_i}) + N_{pred,NCP} \quad (9)$$

where,

$N_{pred,int}$ = expected crash frequency for the intersection (unit: crashes/year);

$N_{pred,NCP}$ = expected NCP crash frequency for the intersection (unit: crashes/year);

N_{pred,CP_i} = expected CP crash frequency for the i^{th} CP (unit: crashes/CP·year);

n = the number of CPs in the intersection (32 CPs for conventional 4SG).

5.3.8.1 Conflict Point SPF

The CP-SPF was estimated using the log-transformed major and minor CMVs as exposure variables and the types of conflict point as categorical variables. The developed model form and parameters are shown in equation below. In this model, α_i indicates the constant for CP types, so the actual model includes three categorical variables: α_{Cross} , $\alpha_{Diverge}$, and α_{Merge} .

The functional form of CP-SPF can also be expressed as a power function. As this model form can satisfy the boundary condition by predicting zero CP crash when either the major or minor CMV is zero, it has been widely used in estimating traditional SPFs (11). Furthermore, the previous studies used the log-transformed AADTs as exposure variables for model improvement by normalizing right-skewed traffic volumes (14, 15).

$$\begin{aligned} N_{pred,CP_i} &= \exp(\alpha_i + \beta_{CMV_{Maj}} \cdot \ln(CMV_{Maj}) + \beta_{CMV_{Min}} \cdot \ln(CMV_{Min})) \\ &= e^{\alpha_i} \cdot (CMV_{Maj})^{\beta_{CMV_{Maj}}} \cdot (CMV_{Min})^{\beta_{CMV_{Min}}} \end{aligned} \quad (10)$$

where,

N_{pred,CP_i} = predicted CP crashes for a CP (unit: crashes/CP·year);

α_i = constant for CP type i (i = crossing, merging or diverging);

β_{CMV} = coefficient for major and minor CMVs;

CMV = major and minor CMVs (unit: veh/day).

5.3.8.2 Non-Conflict Point SPF

The NCP-SPF was estimated using the negative binomial regression model with the log-transformed major and minor AADTs as shown in the equation below. While the CP-SPF predicts the CP-level crashes which are then aggregated at the intersection-level, the NCP-SPF directly predicts the total number of NCP crashes at the intersection-level. The NCP-SPF has same model form to the traditional SPF suggested in the HSM (6).

$$\begin{aligned} N_{pred,NCP} &= \exp(\alpha + \beta_{AADT_{Maj}} \cdot \ln(AADT_{Maj}) + \beta_{AADT_{Min}} \cdot \ln(AADT_{Min})) \\ &= e^{\alpha} \cdot (AADT_{Maj})^{\beta_{AADT_{Maj}}} \cdot (AADT_{Min})^{\beta_{AADT_{Min}}} \end{aligned} \quad (11)$$

where,

- $N_{pred,NCP}$ = predicted NCP crashes for an intersection (unit: crashes/year);
- α = constant;
- β_{AADT} = coefficient for major and minor AADTs (unit: veh/day).

5.4 Data Collection

5.4.1 Site Selection

The crash and traffic volume data were collected from the 35 sites and included 21 conventional four-leg signalized intersections, 11 RCUTs, and 3 DDIs in North Carolina. A list of sample sites is shown in

The crash data were queried and extracted from the Traffic Engineering Accident Analysis System (TEAAS) database using a 150-foot radius from the center point of the conventional intersection. For the AIIIs (RCUTs and DDIs), this study used crashes collected for a prior NCDOT safety project evaluation. For conventional intersections, a similar number of sites were selected for different ranges of AADTs in order to avoid sampling bias in traffic volumes. As AADT is bi-directional, the average of major and minor AADTs in 2017 was considered. The selected conventional intersections include six sites with average AADT under 10,000 veh/day, seven sites with average AADT between 10,000 ~ 20,000 veh/day, and eight sites with average AADT over 20,000 veh/day. For RCUTs, most of them were installed as a series in a row, so they have multiple signalized zones. Therefore, this study regarded each signalized zone as an independent site in the safety analysis. The summary statistics of all the combined data are organized in TABLE 17.

TABLE 16. All the sites are signalized, so all the conflicting movements at crossing CPs are controlled by signals, while some of the merging and diverging CPs are operated without signals. However, as the CP diagram is based on the traffic stream, the number of CPs for the intersection designs do not change by their actual lane configurations or signals. So, this study regarded the merging/diverging CPs with and without a signal as the same in the safety analysis.

The crash data were queried and extracted from the Traffic Engineering Accident Analysis System (TEAAS) database using a 150-foot radius from the center point of the conventional intersection. For the AIIIs (RCUTs and DDIs), this study used crashes collected for a prior NCDOT safety project evaluation. For conventional intersections, a similar number of sites were selected for different ranges

of AADTs in order to avoid sampling bias in traffic volumes. As AADT is bi-directional, the average of major and minor AADTs in 2017 was considered. The selected conventional intersections include six sites with average AADT under 10,000 veh/day, seven sites with average AADT between 10,000 ~ 20,000 veh/day, and eight sites with average AADT over 20,000 veh/day. For RCUTs, most of them were installed as a series in a row, so they have multiple signalized zones. Therefore, this study regarded each signalized zone as an independent site in the safety analysis. The summary statistics of all the combined data are organized in TABLE 17.

TABLE 16 A LIST OF SAMPLE SITES FOR SAFETY DATA COLLECTION

Street Names	Intersection Type	Feature
NW Maynard Rd & High Housing Rd	Conventional 4SG	No Channelized Lane
SE Maynard Rd & Cary Towne Blvd	Conventional 4SG	No Channelized Lane
S Academy St & E Chatham St	Conventional 4SG	No Channelized Lane
SW Cary Pkwy & High House Rd	Conventional 4SG	No Channelized Lane
Willow Rd & E Gate City Blvd	Conventional 4SG	No Channelized Lane
N Harrison Ave & Chapel Hill Rd	Conventional 4SG	No Channelized Lane
Kildaire Farm Rd & SE Maynard Rd	Conventional 4SG	No Channelized Lane
Kildaire Farm Rd & SE Cary Pkwy	Conventional 4SG	No Channelized Lane
E Florida St & Martin Luther King Jr Dr	Conventional 4SG	No Channelized Lane
Lovett St & W Florida St	Conventional 4SG	No Channelized Lane
Coliseum Blvd & W Florida St	Conventional 4SG	No Channelized Lane
W Friendly Ave & New Garden Rd	Conventional 4SG	No Channelized Lane
Muir's Chapel Rd & W Market St	Conventional 4SG	No Channelized Lane
S Holden Rd & Walker Ave	Conventional 4SG	No Channelized Lane
SE Cary Pkwy & Tryon Rd	Conventional 4SG	No Channelized Lane
S Holden Rd & Spring Garden St	Conventional 4SG	Channelized Right Turn Lane
N Dudley St & E Lindsay St	Conventional 4SG	Channelized Right Turn Lane
W Florida St & Freeman Mill Rd	Conventional 4SG	Channelized Right Turn Lane
W Gate City Blvd & Coliseum Blvd	Conventional 4SG	Channelized Right Turn Lane
Tryon Rd & Kildaire Farm Rd	Conventional 4SG	Channelized Right Turn Lane
High House Rd & Davis Dr	Conventional 4SG	Channelized Right Turn Lane
US 17 in Leland - (A) U-Turn	RCUT	U-Turn
US 17 in Leland - (B) US 17 at Grandiflora	RCUT	Crossover
US 17 in Leland - (C) U-Turn	RCUT	U-Turn
US 17 in Leland - (D) US 17 at Gregory Rd	RCUT	Crossover
US 17 in Leland - (E) U-Turn	RCUT	U-Turn
US 17 in Leland - (F) US 17 at Olde Waterford	RCUT	Crossover
US 17 in New Hanover & Pender - US 17 at Futch's Creek Rd	RCUT	Half Crossover
US 17 in New Hanover & Pender - US 17 at SR 1571 (Scott's Hill Loop Rd) (South)	RCUT	Half Crossover
US 17 in New Hanover & Pender - US 17 at SR 1572 (Sidbury Rd)	RCUT	Half Crossover
US 17 in New Hanover & Pender - US 17 at SR 1571 (Scott's Hill Loop Rd) (North)	RCUT	Half Crossover
I-85 - Poplar Tent Rd - (B) Pitts School Rd at I-85	RCUT	Half RCUT
I-85 - Poplar Tent Rd - (C) I-85 & Poplar Tent Rd DDI (North Ramp)	RCUT	DDI - Ramp
I-85 - Poplar Tent Rd - (D) I-85 & Poplar Tent Rd DDI (South Ramp)	RCUT	DDI - Ramp
US 17 at Dawson Cabin - Dawson Cabin Rd at US 17	RCUT	Half T-Intersection

TABLE 17 SUMMARY STATISTICS FOR VARIABLES

Intersection-Level Crash Statistics	Severity	Mean	Std. Dev.	Min - Max	SUM
Total (CP + NCP) Crashes	All	8.97	6.78	0 - 31	1838
	FI	2.76	2.55	0 - 15	566
	PDO	6.20	5.43	0 - 23	1272
CP Crashes	All	2.75	2.43	0 - 13	563
	FI	1.20	1.38	0 - 7	245
	PDO	1.55	1.62	0 - 8	318
NCP Crashes	All	6.22	5.47	0 - 27	1275
	FI	1.57	1.79	0 - 9	321
	PDO	4.65	4.65	0 - 21	954
CP-Level Crash Statistics	Severity	Mean	Std. Dev.	Min - Max	SUM
Total CP Crashes	All	0.10	0.37	0 - 4	563
	FI	0.04	0.23	0 - 3	245
	PDO	0.06	0.25	0 - 3	318
Crossing	All	0.15	0.45	0 - 4	410
	FI	0.08	0.30	0 - 3	205
	PDO	0.08	0.29	0 - 3	205
Merging	All	0.07	0.30	0 - 3	101
	FI	0.02	0.14	0 - 2	28
	PDO	0.05	0.25	0 - 3	73
Diverging	All	0.04	0.20	0 - 2	52
	FI	0.01	0.09	0 - 1	12
	PDO	0.03	0.17	0 - 2	40
Traffic Volume (veh/day) – Arterial Road		Mean	Std. Dev.	Min - Max	SUM
Major AADT		20,904	8,760	6,150 – 43,000	4,285,268
Minor AADT		11,554	7,664	0 – 28,000	2,368,553
Major CMV		5,100	3,056	149 – 21,959	27,927,154
Minor CMV		1,847	1,940	5 – 12,735	10,116,097
CP Type		Coded Dummy Variables (Number of CPs)			
Total Number of CPs		5,477 CPs			
Crossing		1 = Crossing (2,715 CPs); 0 = Otherwise (2,762 CPs)			
Merging		1 = Merging (1,417 CPs); 0 = Otherwise (4,060 CPs)			
Diverging		1 = Diverging (1,345 CPs); 0 = Otherwise (4,132CPs)			

5.4.2 Crash Data

Crash data were collected through the TEASS of the NCDOT. Sample data included yearly crash frequencies and their severities collected from 2010 to 2017. The yearly collected crash data were regarded as unique observations to allow the models to account for the yearly changes in unobserved crash factors and to achieve a large enough sample size for model fitting. To estimate the separate models for severity, the collected crashes were divided into FI and PDO crashes.

5.4.3 Annual Average Daily Traffic (AADT)

For some sample sites, the AADTs were missing for several years as they were collected bi-yearly. The missing AADTs were estimated by the principles suggested in the HSM: the AADTs for intervening years can be estimated by interpolation; the AADTs for years before the first year of available AADT were

assumed to be equal to the first year AADT; and the AADTs for years after the last year of available AADT were assumed to be equal to the last year AADT (6).

5.5 Safety Analysis Results

5.5.1 Model Estimation Results

Three crash frequency models for different severities (TOT model = total crashes, FI model = fatal & injury crashes, and PDO model = property damage only) were estimated. The CP types were used as categorical variables and the intercept term was dropped in the model to avoid the multi-collinearity problem between categorical variables. All the model parameters were estimated by means of maximum likelihood estimation using the generalized linear model with the log link function.

TABLE 18 shows the estimated coefficients and the statistical significance for the independent variables for the estimated models. The results show that all the estimated parameters in three models (TOT, FI, and PDO) are statistically significant at the 95% confidence level, except for the minor CMV in the FI model for the CP-SPF. One possible reason for the less significance for the minor CMV is the limited amount of data which could cause low reliability of estimation. Another possible reason is the cross-model correlation problem due to separate modeling for crash severities (11, 16). All the traffic volume variables (CMVs in the CP-SPF and AADTs in the NCP-SPF) are positively associated with the crash frequency. In the three CP-SPF models (TOT, FI, and PDO), the crossing CP showed relatively higher value than the other two types of diverging and merging CPs. This implies the impact of crossing CP on the crash frequency is higher than other two CP types, which is coincident with the heterogeneity in crash frequency and crash rate between CP types discussed earlier in the previous section of this report.

TABLE 18 MODEL ESTIMATION RESULTS FOR MOVEMENT-BASED SPFS

Movement-Based SPFs	Parameters	TOT Model		FI Model		PDO Model	
		Coefficient	P-value	Coefficient	P-value	Coefficient	P-value
CP-SPF	$\alpha_{CP,Crossing}$	-8.501	***	-8.267	***	-10.160	***
	$\alpha_{CP,Diverging}$	-9.873	***	-10.464	***	-11.073	***
	$\alpha_{CP,Merging}$	-9.316	***	-9.706	***	-10.571	***
	$\beta_{CMV_{Major}}$	0.689	***	0.663	***	0.749	***
	$\beta_{CMV_{Minor}}$	0.109	*	0.015		0.166	**
NCP-SPF	α_{NCP}	-10.874	***	-6.885	***	-13.618	***
	$\beta_{AADT_{Major}}$	0.792	***	0.531	**	0.828	***
	$\beta_{AADT_{Minor}}$	0.521	***	0.229	***	0.742	***

Statistical Significance Codes: '***' < 0.001, '**' < 0.01, '*' < 0.05, '.' < 0.1

In application, the CP and NCP crashes can be predicted for given traffic volumes using the estimated models in the following manner.

For a CP with major CMV of 15,000 veh/day and minor CMV of 8,000 veh/day, the total CP crashes for CP types can be predicted as follows.

- Crossing: $N_{pred,CP} = \exp(-8.501 + 0.689 \times \ln(15,000) + 0.109 \times \ln(8,000)) = 0.41$ crashes
- Diverging: $N_{pred,CP} = \exp(-9.873 + 0.689 \times \ln(15,000) + 0.109 \times \ln(8,000)) = 0.10$ crashes
- Merging: $N_{pred,CP} = \exp(-9.316 + 0.689 \times \ln(15,000) + 0.109 \times \ln(8,000)) = 0.18$ crashes

For an intersection with major AADT of 30,000 veh/day and minor AADT of 15,000 veh/day, the total NCP crashes can be predicted as follows.

$$- N_{\text{pred,NCP}} = \exp(-10.874 + 0.792 \times \ln(30,000) + 0.521 \times \ln(15,000)) = 9.98 \text{ crashes}$$

To calculate the predicted total intersection crashes, the analyst would need to calculate the CP crashes for each individual conflict point using the method above along with the total NCP crashes.

5.5.2 Cumulative Residuals (CURE) Plot

The statistical significance of estimated coefficients does not sufficiently prove the estimated SPF models are appropriate in crash prediction. For practical use, the models need to be examined to determine if they provide unbiased prediction for the entire range of exposure variables by drawing the plots for cumulative residuals (CURE) between the observed crashes and predicted crashes (17). This validation effort drew CURE plots for the TOT, FI, and PDO models of MB-SPFs using the average crash frequency and AADTs per year for the sample sites.

FIGURE 15 represents the CURE plots for the intersection-level total crashes. The Y-axis is the CURE, and the X-axis is the major AADT in the first-row graphs, the minor AADT in the second-row graphs, and the fitted total crashes in the third-row graphs.

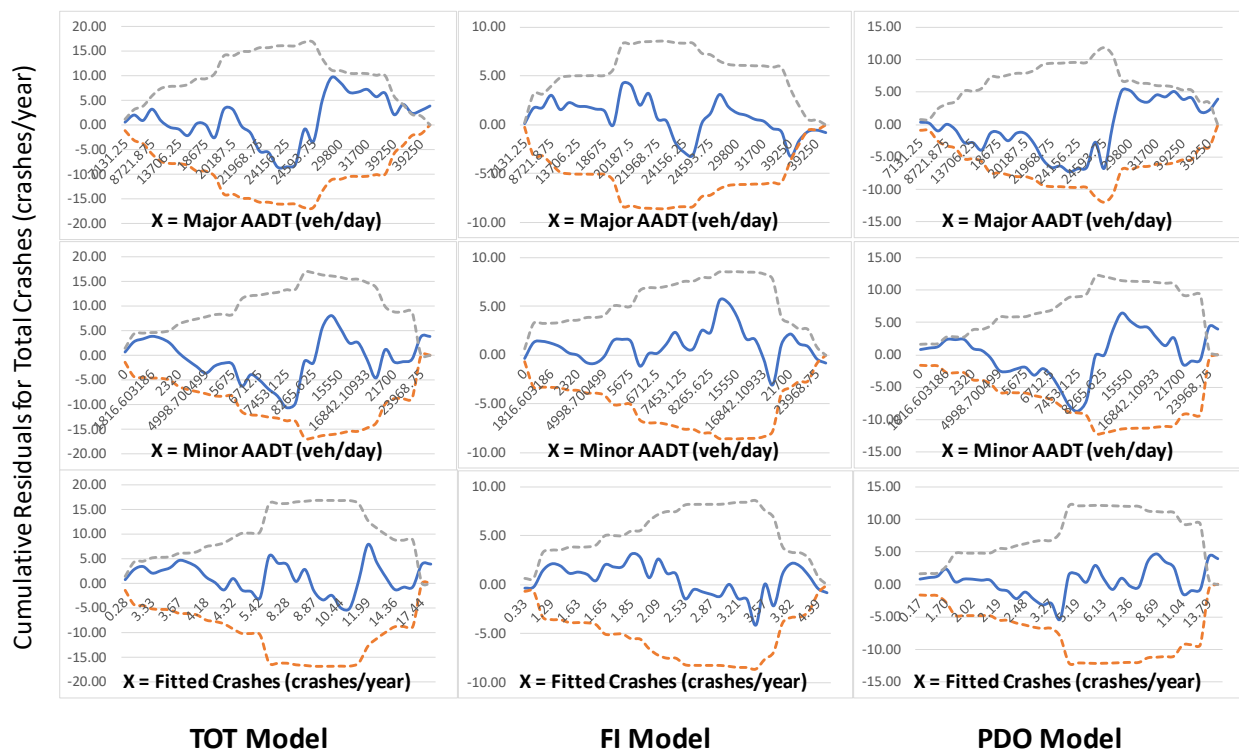


FIGURE 15 CUMULATIVE RESIDUALS (CURE) PLOTS FOR TOTAL CRASHES PREDICTED BY MB-SPFs

In the CURE plots, we could verify the absence of bias in prediction by examining if the CURE oscillates around the horizontal axis within the confidence limits of $\pm 2\sigma$ (17). The solid line is the CURE, and the upper and lower dashed lines represent the $+2\sigma$ and -2σ confidence limits. The drawn CURE plots show most of cumulative residuals stay within the confidence limits. The result showed the estimated models have some prediction bias for some range of exposure variables and fitted crash frequency, but they are

not statistically significant as the CUREs oscillate mostly within the upper and lower boundaries. For a small portion of CUREs outside of limits, it could be improved by increasing the number of sample sites, modifying the model forms, and including additional independent variables (11).

5.5.3 Crash Prediction Results for Designed Volume Scenarios

Based on the estimated MB-SPFs, this study compared the relative safety performance between intersection designs. Considering the NCP-SPF used AADT and, thus, predicted the same amount of NCP crashes regardless of the design, it is more appropriate to compare the total predicted CP crashes as a relative safety performance between intersection designs.

As such, this study compared the aggregated CP crashes on the major (E-W) road between the seven grade-separated intersection designs for sixteen design volume scenarios, and the results are shown in Table 19. The figures in the table are the aggregated CP crashes for multiple CPs on the major (E-W) road for the intersection designs. The prediction results for the conventional intersection are also provided as reference. The results for the conventional intersection are the aggregated CP crashes for the entire intersection (all approaches) since it is not separated into the major and minor roads. The deep red cell indicate the higher CP crashes indicating poor safety performance and the deep green indicates the lower CP crashes, indicating better safety performance. Like the macroscopic operational analysis results, we can compare the relative safety performance between designs for each scenario.

TABLE 19 PREDICTED CP CRASHES FOR INTERSECTION DESIGNS FOR 16 VOLUME SCENARIOS (MAJOR (E-W) ROAD)

Scenario	Approach Volume	Movement Volume		Base*	DL-D	DL-U	SPL	RCUT (U-R)	Contra-RCUT	RCUT (R-U)	QUA (SE)
		EB	WB	Conventional							
EBN-WBN	EB: 50% WB: 50%	N	N	7.815	2.19	2.06	2.02	1.51	1.45	1.50	2.13
EBT-WBN		T	N	7.936	2.21	2.10	2.07	1.53	1.48	1.54	2.25
EBL-WBN		L	N	7.810	2.28	2.04	2.01	1.52	1.44	1.46	2.03
EBLT-WBN		LT	N	7.905	2.25	2.08	2.05	1.53	1.47	1.50	2.13
EBT-WBT		T	T	8.053	2.20	2.12	2.09	1.54	1.50	1.57	2.15
EBL-WBT		L	T	7.936	2.28	2.08	2.05	1.54	1.47	1.50	1.96
EBLT-WBT		LT	T	8.027	2.25	2.11	2.09	1.55	1.50	1.54	2.06
EBT-WBL		T	L	7.936	2.28	2.08	2.05	1.54	1.47	1.50	2.33
EBN-WBN	EB: 60% WB: 40%	N	N	7.683	2.17	2.03	2.00	1.48	1.42	1.48	2.29
EBT-WBN		T	N	7.849	2.16	2.06	2.04	1.50	1.46	1.53	2.40
EBL-WBN		L	N	7.706	2.22	1.98	1.95	1.47	1.40	1.43	2.16
EBLT-WBN		LT	N	7.786	2.21	2.03	2.01	1.49	1.43	1.48	2.29
EBT-WBT		T	T	7.937	2.16	2.08	2.06	1.51	1.47	1.55	2.36
EBL-WBT		L	T	7.803	2.22	2.00	1.97	1.47	1.41	1.45	2.12
EBLT-WBT		LT	T	7.879	2.20	2.05	2.03	1.50	1.45	1.50	2.24
EBT-WBL		T	L	7.876	2.23	2.06	2.04	1.52	1.46	1.50	2.45

*The base case was provided for general but not direct numerical comparison to other designs shown. The base conventional intersection must include all movements as the N-S movements conflict with E-W traffic. All other designs show half of the intersection as each design can be combined with a separate design for N-S.

Overall, the three types of RCUTs, including RCUT (U-R), Contra-RCUT, and RCUT (R-U), showed the best performance compared to other designs. On the contrary, the QUA (SE) and DL-D show relatively poor safety performance. While the operational macroscopic analysis showed all the designs have poor performance in the heavy left turn movement scenarios, the safety performance over the 16 volume scenarios did not fluctuate significantly. For example, the difference between the maximum and minimum CP crashes for the DL-D is 0.12 (= 2.28 – 2.16). This is because the total (EB+WB) volume is constant, and so, the conflicting movement volumes on each CP did not change significantly using varying volume scenarios. When comparing the predicted CP crashes between the designs, the differences between the maximum and minimum CP crashes for the volume scenarios are between 0.70 and 0.99. For example, for volume scenario 16, the difference in CP crashes between Contra-RCUT and QUA (SE) is the 0.99 (= 2.45 – 1.46). This difference in CP crashes between designs will increase at the intersection-level, if we assume the same designs for both major and minor roads (e.g. Contra-RCUT & Contra-RCUT vs. QUA (SE) & QUA (SE)).

5.5.4 An Example of Crash Prediction Using MB-SPFs

To facilitate the practical use, this section provides the details of crash prediction process using MB-SPFs step-by-step. For an example analysis, the DL-D design was assumed for both major and minor roads, which is called the DL-D combination design in this section.

5.5.4.1 Traffic Volume Inputs

As a first step, the traffic volume inputs need to be determined. The base volume scenario (scenario 1: EBN-WBN) was used for the example analysis. Same with the operational macroscopic analysis, the EB & WB road and NB & SB road were assumed major and minor roads, respectively. The traffic volume inputs were determined according to the assumptions and default parameter values stated in the section 4.2.4. For instance, the minor (N-S) road total volume was set to half of that of the major (E-W) road. And, for the minor road, the normal turning movement proportion (left turn of 15%, through of 70%, and right turn of 15%) was assumed. Figure 16 shows traffic volume inputs used for the example analysis. It should be noted that the volumes in the figure represent the daily volume.

Equivalent Passenger Car Volume				
	Volume (Veh/Day)			
	U-Turn 	Left 	Thru 	Right 
Eastbound	0	4500	21000	4500
Westbound	0	4500	21000	4500
Southbound	0	2250	10500	2250
Northbound	0	2250	10500	2250

FIGURE 16. TRAFFIC VOLUME INPUTS FOR THE EXAMPLE ANALYSIS

5.5.4.2 Conflict Point Diagram

The conflict point diagram for the intersection design of interest needs to be drawn. Figure 17 shows the conflict point diagram for the DL-D combination design. Some movements in the middle of the figure were drawn like conflicting each other, but no CPs were drawn, since those movements are actually grade-separated.

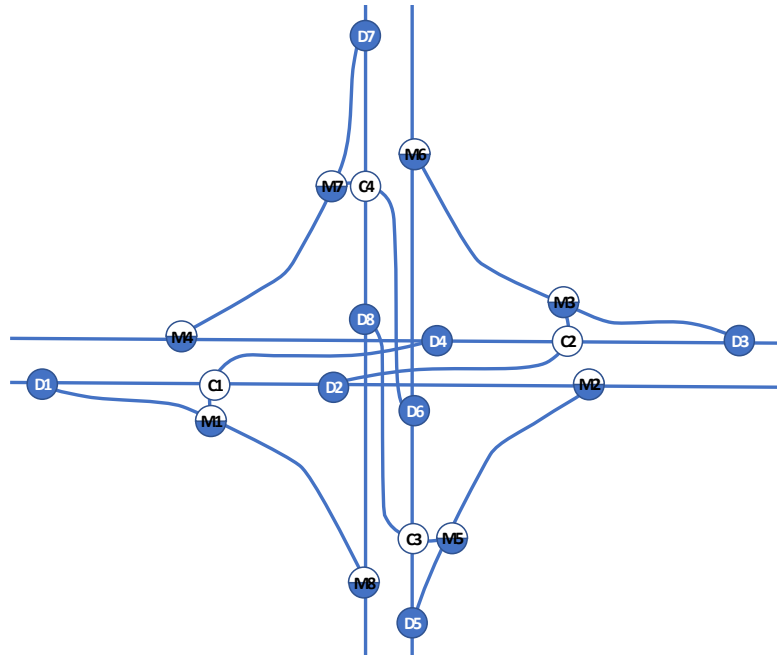


FIGURE 17. CONFLICT DIAGRAM FOR DIRECT LEFT - DOWNSTREAM (DL-D) COMBINATION DESIGN

5.5.4.3 Conflict Movement Volumes

Based on the drawn conflict point diagram and the traffic volume inputs, the conflict movement volumes (CMVs) need to be calculated for the CPs. For example, the diverging CP where the Eastbound through and right turn movements conflict was coded D1 in Figure 17. At the D1, the actual conflicting volumes can be calculated as the (EBT+EBL) of 25,500 (= EBT (21,000) + EBL (4,500)) and EBR of 4500 (unit: veh/day). The major and minor CMVs were determined by the traffic volumes. The higher and lower volumes were determined to the major and minor CMVs, respectively. In this case, the (EBT+EBL) is the major CMV and the (EBR) is the minor CMV.

5.5.4.4 Crash Prediction

The CP and NCP crashes can be predicted using the model estimation results in Table 18. This section provides the details in the CP and NCP crash prediction for the DL-D combination design. The CP crash prediction calculations are provided for the three sample CPs of C1, M1, and D1, shown in Figure 17. The details are as follows.

For the intersection of DL-D combination design with the major AADT of 60,000 veh/day and the minor AADT of 30,000 veh/day, the CP crashes for the C1, M2, and D1, and the NCP crashes were calculated by the MB-SPFs as follows. For the CP crash prediction, the major and minor CMVs were calculated based on the movements conflicting at a CP.

- C1 (Crossing)

$$N_{\text{pred,CP}} = \exp(\alpha_{CP,Crossing} + \beta_{CMV_{Major}} \times \ln(EBT + EBL) + \beta_{CMV_{Minor}} \times \ln(WBL))$$

$$= N_{\text{pred,CP}} = \exp(-8.501 + 0.689 \times \ln(25,500) + 0.109 \times \ln(4,500)) = 0.55 \text{ crashes}$$

- M1 (Merging)

$$N_{\text{pred,CP}} = \exp(\alpha_{CP,Merging} + \beta_{CMV_{Major}} \times \ln(EBR) + \beta_{CMV_{Minor}} \times \ln(WBL))$$

$$= N_{\text{pred,CP}} = \exp(-9.316 + 0.689 \times \ln(4,500) + 0.109 \times \ln(4,500)) = 0.07 \text{ crashes}$$

- D1 (Diverging)

$$N_{\text{pred,CP}} = \exp(\alpha_{CP,Crossing} + \beta_{CMV_{Major}} \times \ln(EBT + EBL) + \beta_{CMV_{Minor}} \times \ln(EBR))$$

$$= N_{\text{pred,CP}} = \exp(-9.873 + 0.689 \times \ln(25,500) + 0.109 \times \ln(4,500)) = 0.14 \text{ crashes}$$

- NCP Crashes

$$N_{\text{pred,NCP}} = \exp(-10.874 + 0.792 \times \ln(60,000) + 0.521 \times \ln(30,000)) = 24.79 \text{ crashes}$$

In a similar way, the CP crashes for the other CPs were predicted by the MB-SPFs using the major and minor CMVs. The conflicting movements, major and minor CMVs, and the predicted CP crashes for the CPs, predicted NCP crashes, and the predicted total crashes are presented in TABLE 20. The prediction results showed the 28.29 total crashes per year with the 3.50 CP crashes and 24.79 NCP crashes.

TABLE 20. CRASH PREDICTION RESULTS FOR THE EXAMPLE ANALYSIS

Road	CP Code	CP Type	Movement ₁	Movement ₂	CMV _{Maj} (veh/day)	CMV _{Min} (veh/day)	Predicted Crashes (crashes/year)		
							CP	NCP	Total
SUM	-	-	-	-	-	-	3.50	24.79	28.29
E-W	D1	Diverging	EBT+EBL	EBR	25500	4500	0.14		
E-W	M1	Merging	EBR	WBL	4500	4500	0.07		
E-W	C1	Crossing	EBT+EBL	WBL	25500	4500	0.55		
E-W	D2	Diverging	EBT	EBL	21000	4500	0.12		
E-W	M2	Merging	EBT	NBR+SBL	21000	4500	0.21		
E-W	D3	Diverging	WBT+WBL	WBR	25500	4500	0.14		
E-W	M3	Merging	WBR	EBL	4500	4500	0.07		
E-W	C2	Crossing	WBT+WBL	EBL	25500	4500	0.55		
E-W	D4	Diverging	WBT	WBL	21000	4500	0.12		
E-W	M4	Merging	WBT	SBR+NBL	21000	4500	0.21		
N-S	D5	Diverging	NBT+NBL	NBR	12750	2250	0.08		
N-S	M5	Merging	NBR	SBL	2250	2250	0.04		
N-S	C3	Crossing	NBT+NBL	SBL	12750	2250	0.32		
N-S	D6	Diverging	NBT	NBL	10500	2250	0.07		

N-S	M6	Merging	NBT	WBR+EBL	10500	9000	0.14		
N-S	D7	Diverging	SBT+SBL	SBR	12750	2250	0.08		
N-S	M7	Merging	SBR	NBL	2250	2250	0.04		
N-S	C4	Crossing	SBT+SBL	NBL	12750	2250	0.32		
N-S	D8	Diverging	SBT	SBL	10500	2250	0.07		
N-S	M8	Merging	SBT	EBR+WBL	10500	9000	0.14		

5.6 Limitations in Safety Analysis

5.6.1 Limitation in Crash Data Classification

The proposed method based on MB-SPFs has a potential misclassification issue with the crash classification. During data collection, crashes were classified based on the travel directions and vehicle maneuvers without a review of individual crash reports. Therefore, the classified crash dataset contains potential misclassification issues due to miscoded information by police officers. Also, in the data processing, the diagonal directions (e.g. Southwest or Southeast) were oversimplified to a straight compass direction (e.g. South). This oversimplification could result in misclassifying the conflict type and with the default categorization of non-conflict point crash types, excess NCP crashes could be recorded. These limitations imply a review of the individual crash report would be beneficial to ensure the correct classification of crashes.

5.6.2 Limited Sample Sites

The sample sites for the crash data collection was limited to specific types of intersections (conventional intersections, RCUTs, and DDIs). It should be noted that CP (crossing, merging, and diverging) crashes and NCP crashes may have different characteristics, such as the crash rates and/or distributions for severities, in different designs of intersections when their geometry and operation can confuse drivers. Therefore, the proposed models are expected to be improved by adding additional sample crashes with more varied intersection designs in future studies.

6 Conclusions

This study developed operational and safety performance evaluation methodologies for the grade-separated intersection and compared the analysis results between seven designs with different left turn treatments. For the operational performance analysis, the critical movement analysis method was used for the *macroscopic analysis* and the overall critical v/c ratio on the major (E-W) road was compared as a performance measure. As the purpose of macroscopic operational analysis was to compare the performance between the designs, the same amount of total (EB+WB) volume was used for all seven designs. The results showed the DL-D, DL-U, and SPL have relatively better operational performance than others over the 16 volume scenarios. In the *microscopic analysis*, the different amounts of total (EB+WB) volumes were used for designs in order to compare the performance of each design between various traffic conditions. VISSIM 10.0 was used with average delay reported using ten repeated simulations for sixteen volume scenarios. The results showed DL-D, SPL, and RCUT (U-R) commonly have poor performance in the scenarios with the EB heavy left turn movement.

For the safety performance analysis, this study proposed a novel concept of crash prediction, movement-based SPF's, which predict the CP and NCP crashes separately using two different models. The process of crash data classification, model development, and estimation results were discussed in detail. The CP crashes predicted for the sixteen volume scenarios were provided as a performance

measure and compared between the seven grade-separated intersection designs. It should be noted that we can compare the relative safety performance between the designs, since the results only includes CP crashes on the major (E-W) road, not the total crashes for an intersection. According to the CP crash prediction results, three types of RCUTs including RCUT (U-R), Contra-RCUT, and RCUT (R-U) are recommended as the designs with better safety performance.

In application, an engineer or planner should consider a variety of qualitative considerations in addition to the operational and safety performance suggested in this study. Chapter 3 discusses many of these considerations which must be weighed against ideal operating or safety conditions. Overall there is no perfect design to address all potential issues but the qualitative summary and the operational and safety models developed can be applied for specific volume conditions and design constraints in order to select one or more grade-separated intersection designs for further analysis.

6.1 Implementation and Future Research

The deliverables associated with this research are ready for use by NCDOT staff and their consultants for including these new grade-separated intersection designs in the preliminary design phase of projects. That said, the research team has identified a set of desirable next steps for additional implementation and future research topics listed below.

Implementation: Training for NCDOT Staff and Consultants on Grade-Separated Intersections

The introduction of new designs presented in this research project does not add tremendous change to the alternative's analysis methodology, but a short (2.5 hour) training course for engineers would enable the greatest benefits to be achieved by NCDOT. This training would introduce the design types, the additional operational outputs for grade-separated intersections, as well as the safety analysis methodology and results. NCDOT Congestion Management can recommend the ideal number of courses and total number of participants, and the team estimates 2 months to develop the course materials and schedule the courses. Another option could use internal resources.

Implementation: Localized Version of CAP-X for NCDOT

There are multiple usability and consistency features which can be added CAP-X that were outside of the scope of the research project. First, the safety analysis methodology can be extended to the existing base designs available in FHWA's CAP-X 3.0. This would allow for a direct planning-level safety comparison using the same conflict point based safety performance functions. Additional user interface improvements could streamline the analysis procedure and allow for grade-separated intersections to be considered in the summary results ranking. CAP-X provides a number of inputs or adjustment factors which have default values, but also has room for additional operational inputs. Capacity for each turning movement type is needed, and there is some general guidance on national defaults, however limited local research in North Carolina has identified very different saturation flow rates compared to the defaults. Other research projects have identified issues with lane utilization at intersections with auxiliary through lanes. These additions would provide more North Carolina-specific outputs and consistency for NCDOT and their contractors using the tool.

Research: Movement-Based Safety Performance Functions

The safety methodology developed in this project has received extremely positive reviews by staff, external safety engineers, as well as national research committees. The current method includes only

signalized control and for a limited combination of geometries that applied to the grade-separated intersection designs. Also, the NCP crash prediction model could be further improved by considering additional independent variables and model forms. In order to expand the methodology and allow for more accurate safety predictions outside of this narrow context, further research is recommended to collect additional safety and turning movement data at a wide variety of intersection types. Also, the proposed method has a potential to be improved by adding additional crash data from more varied types of intersections in future studies. Moreover, it is recommended to classify the crashes based on a review of individual crash reports to prevent potential misclassification issues due to miscoded crashes by police officers and oversimplification of travel directions. The large scale and scope of this study would most likely benefit from funding at the federal level or through a pooled fund project.

Research: Traffic Control Strategies at Grade-Separated Intersections

The project identifies the operational benefits available to grade-separated intersections by limiting the number of critical phases and interaction of opposing flows; however, no research is available to give recommendation on signalization options for these designs. While ideally the two roadways operate independently, coordination between certain movements on both roadways may mitigate issues with spillback on ramps or operating high volume grade-separated quadrants. Research is recommended to identify particularly difficult designs or volume conditions to develop signalization strategies.

References

1. Rodegerdts et al. (2004). Signalized intersections: informational guide (No. FHWA-HRT-04-091).
2. Lochrane, T., Bared, J., & Zhang, W. (2011). Capacity Analysis for Planning of Junctions (CAP-X). FHWA, US Department of Transportation, 2.
3. Sangster, J., & Rakha, H. (2014). Implications of CAP-X: Operational Limitations of Alternative Intersections (No. 14-3794).
4. Hughes, W., Jagannathan, R., Sengupta, D., & Hummer, J. (2010). Alternative intersections/interchanges: Informational report. Washington, DC.
5. Rodegerdts, L. A., Nevers, B. L., Robinson, B., Ringert, J., Koonce, P., Bansen, J., ... & Neuman, T. (2004). Signalized intersections: informational guide (No. FHWA-HRT-04-091). United States. Federal Highway Administration.
6. AASHTO. (2010). Highway Safety Manual. American Association of State Highway and Transportation Officials (AASHTO), Washington, D.C.
7. Hauer, E., J. C. Ng, and J. Lovell. Estimation of safety at signalized intersections. *Transportation Research Record: Journal of the Transportation Research Board*, 1988. 1185: 48-61.
8. Rodegerdts, L. A., B. L. Nevers, B. Robinson, J. Ringert, P. Koonce, J. Bansen, T. Nguyen, J. McGill, D. Stewart, J. Suggett, and T. Neuman. Signalized intersections: informational guide. Publication FHWA-HRT-04-091. FHWA, U.S. Department of Transportation, 2004.23
9. Barron, D. N. The analysis of count data: Overdispersion and autocorrelation. *Sociological methodology*, 1992. 179-220.
10. Cox, D. R. Some remarks on overdispersion. *Biometrika*, 1983. 70(1): 269-274.
11. Srinivasan, R., and K. Bauer. Safety performance function development guide: Developing jurisdiction-specific SPFs. Publication FHWA-SA-14-005, FHWA, U.S. Department of Transportation, 2013.
12. Dean, C., and J. F. Lawless. Tests for detecting overdispersion in Poisson regression models. *Journal of the American Statistical Association*, 1989. 84(406): 467-472.
13. Miaou, S. P. The relationship between truck accidents and geometric design of road sections: Poisson versus negative binomial regressions. *Accident Analysis & Prevention*, 1994. 26(4): 471-482.
14. Lee, T., Y. Y. Choi, S. Y. Kho, and D. K. Kim. Multilevel model for ramp crash frequency that reflects heterogeneity among ramp types. *KSCE Journal of Civil Engineering*, 2018. 22(1): 311-319.
15. Brimley, B. K., M. Saito, and G. G. Schultz. Calibration of Highway Safety Manual safety performance function: development of new models for rural two-lane two-way highways. *Transportation Research Record: Journal of the Transportation Research Board*, 2012. 2279(1): 82-89.
16. Lord, D., and F. Mannering. The statistical analysis of crash-frequency data: a review and assessment of methodological alternatives. *Transportation research part A: policy and practice*, 2010. 44(5): 291-305.
17. Hauer, E. *The art of regression modeling in road safety*. New York: Springer, New York, 2015.

Appendix A: Grade-Separated Intersection Designs with Different Left turn Treatments

Appendix B: Patent Review – Full Report

Appendix C: Graphs for Macroscopic Operational Analysis Results

Appendix D: Turning Movement Volume Proportions